CHARGED PARTICLE DETECTORS USED IN SPACE RESEARCH

Berndt Klecker

Max-Planck-Institut für extraterrestrische Physik

D-85741 Garching, Germany

WRMISS Workshop

At The University Cath. Louvain (UCL)

September 7, 2000

OVERVIEW

1. Introduction

2. In Situ Measurements

2.1 The Parameter Range

2.2 Low Energy Plasma Measurements

2.3 High Energy Plasma Measurements ($\leq$ 300 keV)

2.4 Measurements of Energetic Ions and Electrons at MeV Energies

3. Remote-Sensing Measurements

3.1 Ground Observations (e.g. EISCAT)

3.2 Imaging with Light, UV, X-rays, and Energetic Neutral Atoms

4. Present and Future Developments

4.1 Multispacecraft Mission Concepts (Microsats and Nanosats)

4.2 Sensor Concepts for Micro- and Nanosats

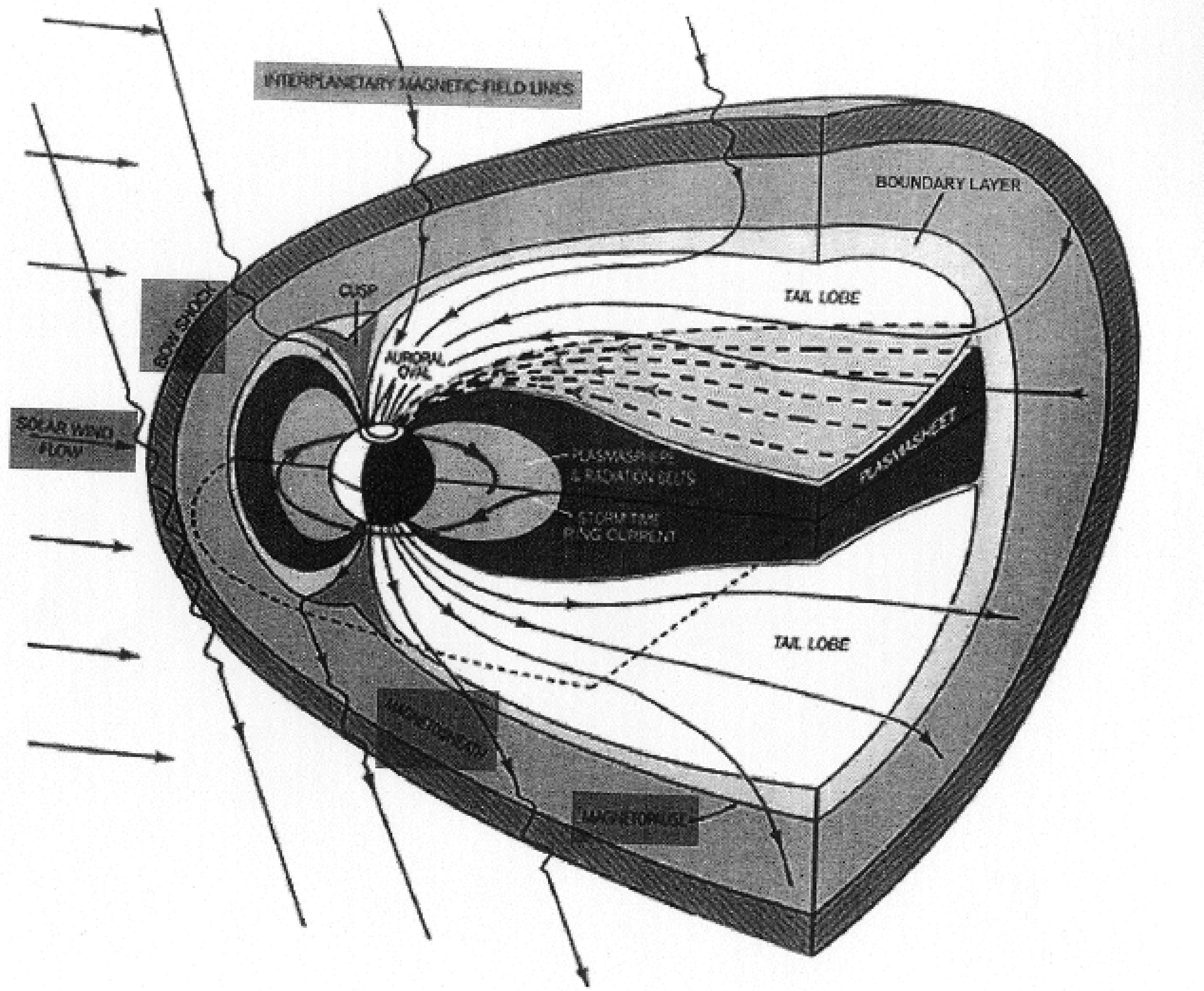
INTERPLANETARY MAGNETIC FIELD LINES
BOUNDARY LAYER
CUSP
TAIL LOBE
AURORAL OVAL
BOW SHOCK
SOLAR WIND FLOW
PLASMASHEET
PLASMASPHERE & RADIATION BELTS
STORM TIME RING CURRENT
TAIL LOBE

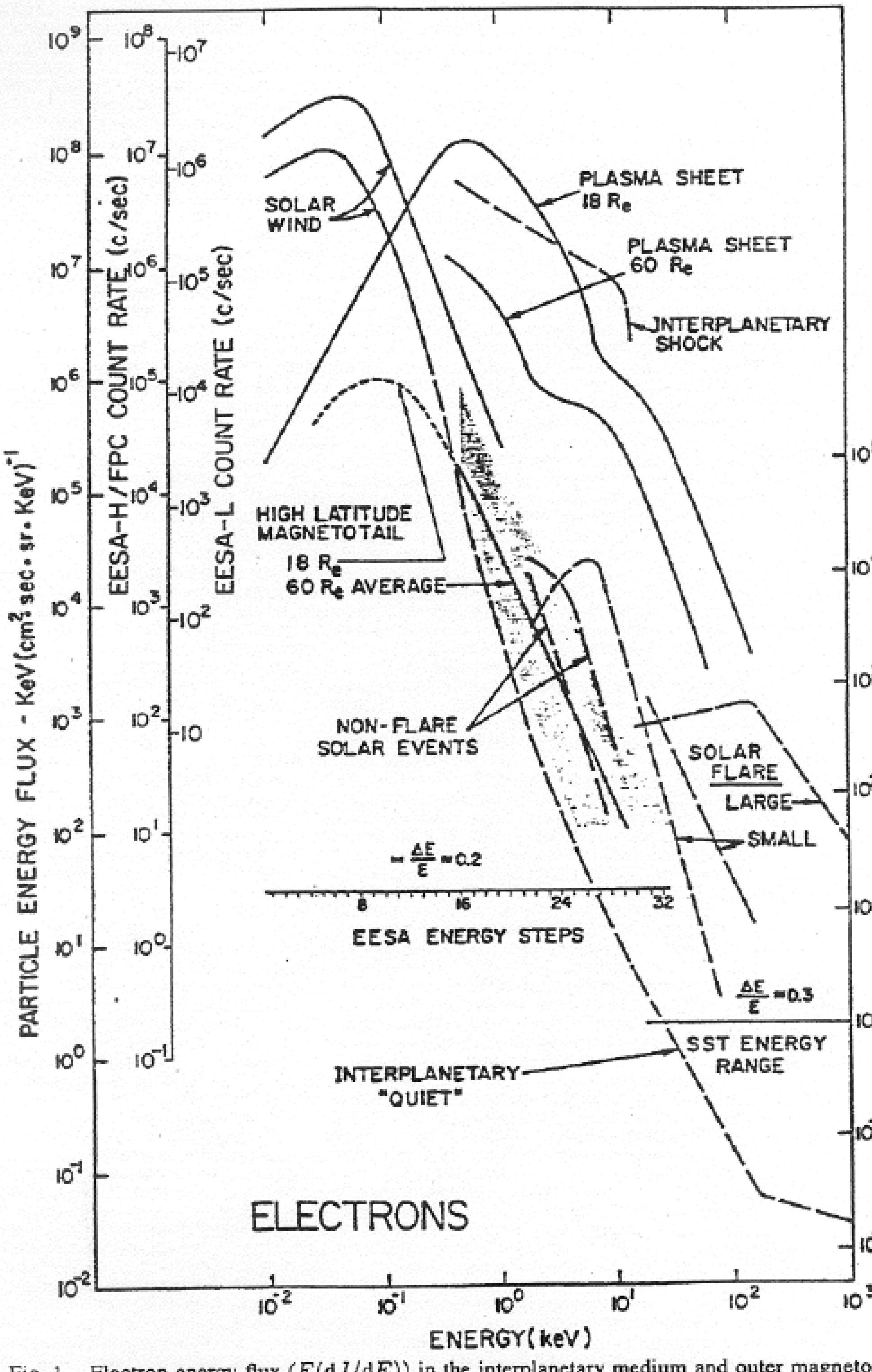

Fig. 1. Electron energy flux ($E(\mathrm{d}J/\mathrm{d}E)$) in the interplanetary medium and outer magnetosphere. Counting rates per channel for the EESA and SST are indicated on the left and right axes, respectively.

Lin et al., 1995

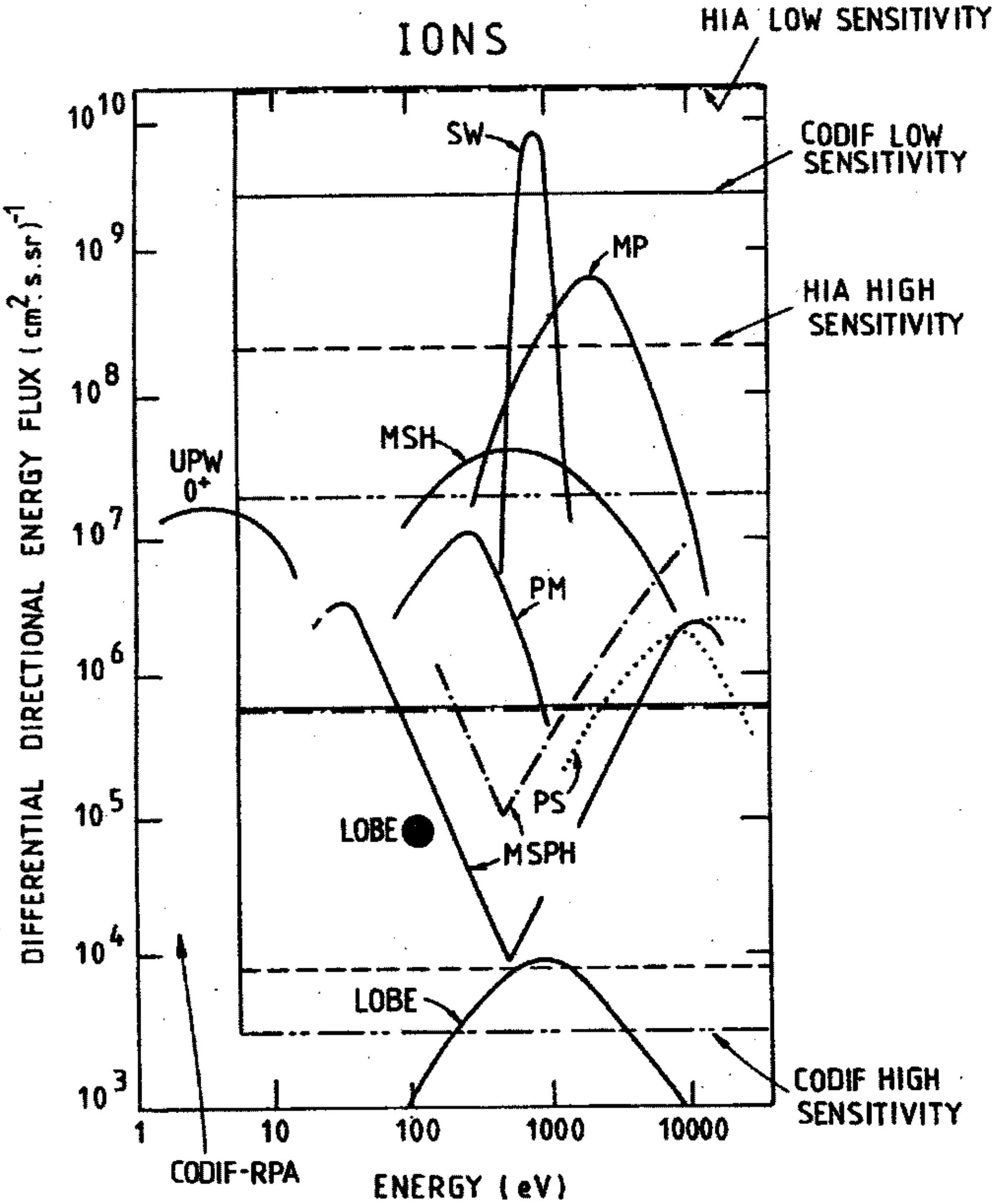

Representative Ion Differential Energy Fluxes in Various Regions of the Magnetosphere of the Earth (Rème et al., 1997)

IN SITU MEASUREMENTS

For the full information we would need to measure:

- Distribution and Composition of Ions in Energy, Space and Time
- Distribution of Electrons in Energy, Space and Time

THE FIRST STEP: COUNTING PARTICLES

Geiger-Müller Counters (GM) and Scintillation Counters (SC) ($e > 100$ keV, $p > 30$ MeV)

Explorer 1	January	1958	
Explorer 3	March	1958	Discovery of Trapped Radiation (e, p ?)
Sputnik 3		1958	
Explorer 4		1959	Trapped Radiation are $p > 30$ MeV

DISCOVERY OF THE RADIATION BELTS

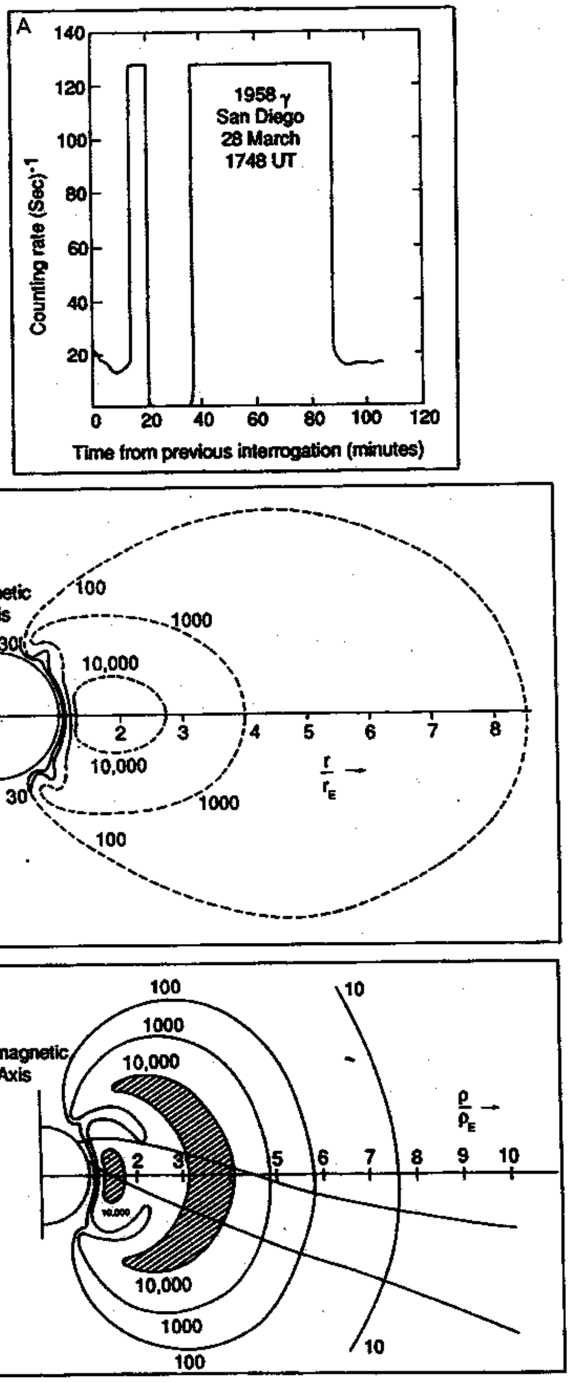

Van Allen et al., 1958, Van Allen and Frank, 1959 (from Williams 1990)

THE LANGMUIR PROBE

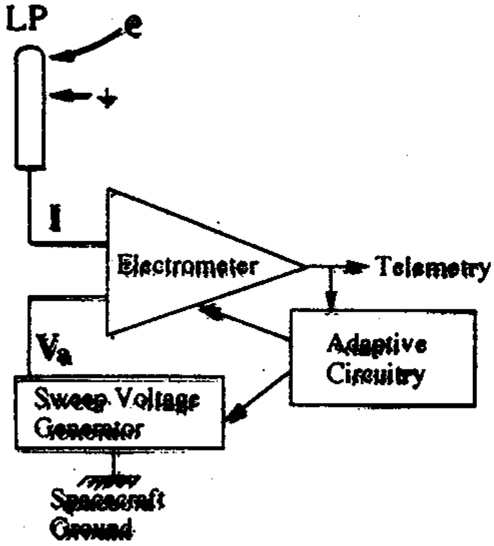

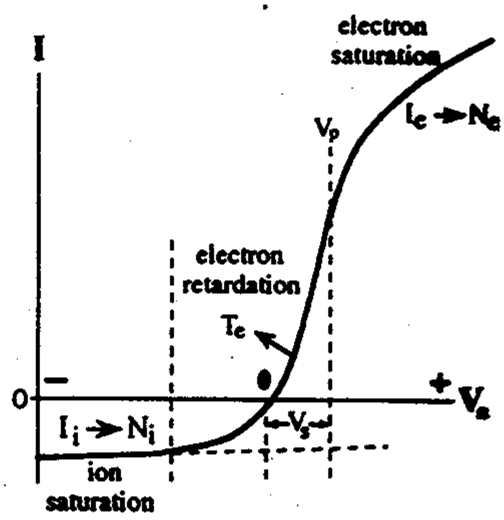

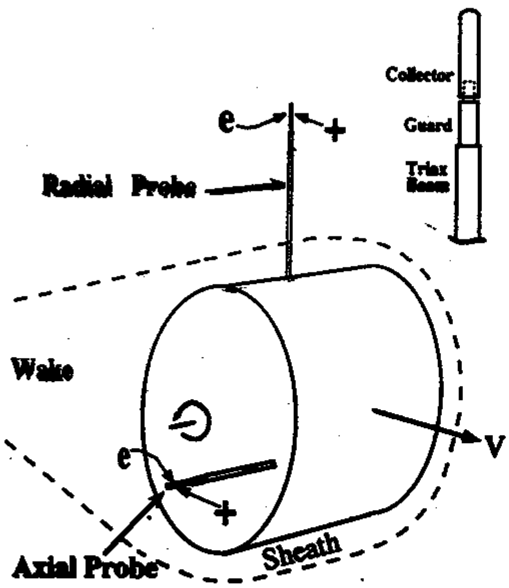

Figure 1. A typical LP arrangement. Two cylindrical probes are mounted on solid triaxial booms. The radial probe is oriented perpendicular to the spin axis and the axial probe is parallel to the spin axis. Both probes are oriented perpendicular to the velocity vector when the spacecraft is despun.

(Brace, 1997)

Measured Parameter:

U-I Characteristic

Inferred Parameters

<u>Ion Density</u> (from Ion Saturation Current I_i)

$$I_i = A\, N_i\, q_i\, v_i / \pi * (1 + kT_i / m_i v_i^2 + 2eV / m_i v_i^2)^{0.5}$$

<u>Electron Temperature</u> (from retardation region)

$$I_e = A\, N_e\, e\, (kT_e / 2\pi m_e)^{0.5} \exp(eV/kT_e)$$

<u>Electron Density</u> (from electron saturation current I_e)

$$I_e = N_e\, A\, e\, 2\, \pi^{-0.5}\, (kT_e / 2\pi m_e)^{0.5}\, (1 + eV/kT_e)^{0.5}$$

First Application in Space in 50s and 60s:

In Thermosphere, Ionosphere (e.g. Tiros-7, Explorer 17, 22)

Modern Application:

SPEDE package onboard SMART-1 (ESA, **S**mall **M**ission for **A**dvanced **R**esearch and **T**echnology)

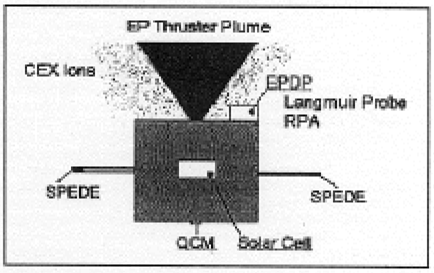

THE RETARDING POTENTIAL ANALYZER

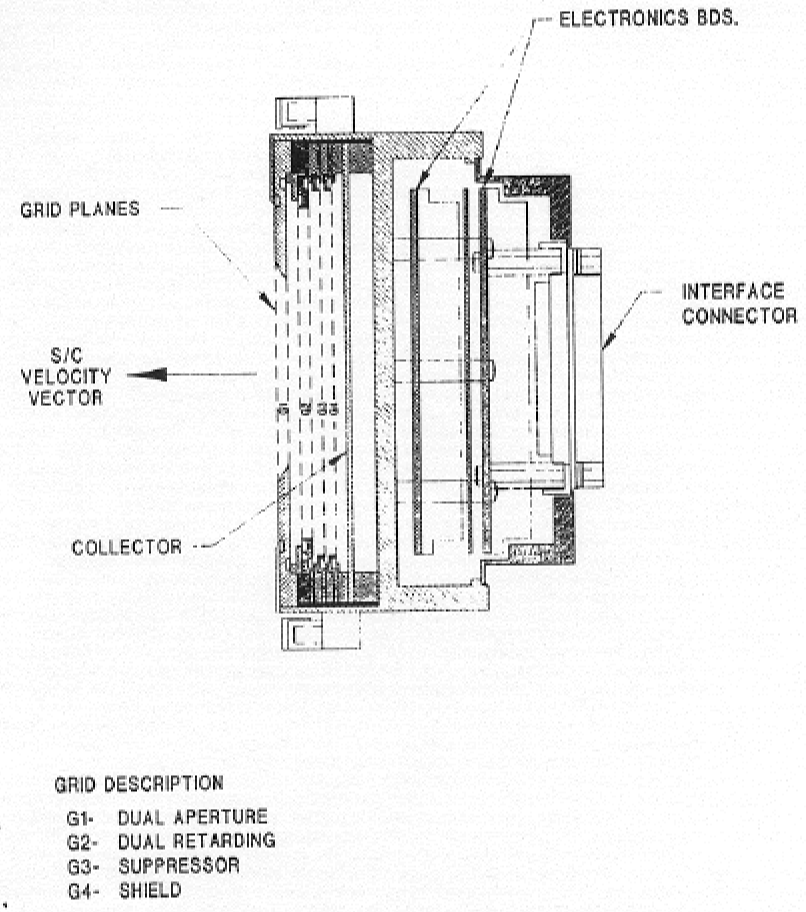

RPA SENSOR CROSS-SECTION

Figure 1. Schematic cross-section of the planar RPA sensor illustrating the arrangement of internal grids required to perform the retarding potential analysis of thermal ions.

$$j_i(P) = 1/2\, \mathbf{N_i}\, V_r\, (1 + \mathrm{erf}(\beta_i f_i) + 1/(\sqrt{\pi}\, \beta_i V_r)\, \exp(-\beta_i^2 f_i^2))$$

$P = q\,(U_r + U_s)$; U_r / U_s: grid / spacecraft potential,

Ni density $\beta_i = (m_i/2kT_i)^{0.5} \sim 1/v_{th}$

V_r velocity $f_i = V_r - (2P/m_i)^{0.5}$

(from Heelis and Hanson, 1997)

CURVED PLATE ANALYZER (CPA)

Energy / Charge Analysis with Electrostatic Deflection

(Spherical-Section Analyzer)

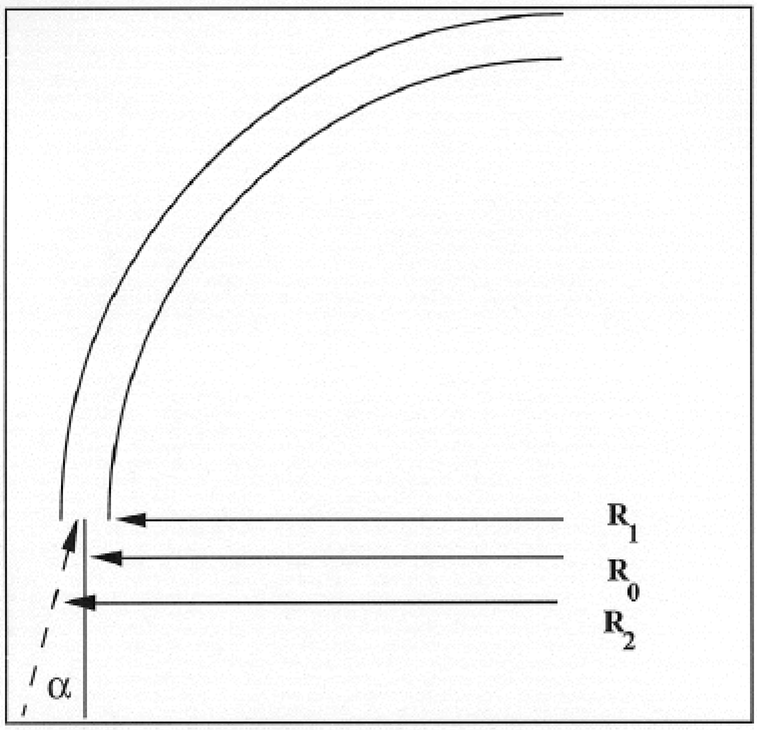

Definitions:

T		Energy of Particle
q		Ionic Charge
$V_{1,2}$		Potential of Plates 1 and 2
V	=	$V_2 - V_1$
ΔR	=	$R_2 - R_1$
R_c	=	$(R_2 + R_1) / 2$
$\phi(r)$		Potential between plates
$E(r)$		Electric field between plates
$\phi(r)$		$= -K / r + \phi_{-}$, with $K = V R_1 R_2 / \Delta R$

For V2 = 0, V = - V1:

$\phi(r) \quad = \quad V (1/r - 1/R_2) / (1/R_1 - 1/R_2) = \Delta V (R_2 - r) R_1 / \Delta R / r$

$E(r) \quad = \quad V R_1 R_2 / \Delta R / r^2$

CURVED PLATE ANALYZER (CPA)

Conditions for Transmission, I. Special Case ($\alpha=0$):

$2\,T / R_0 \quad = \quad q\ E(R_0)$

$T \quad = \quad 0.5\ q\,V\,R_1 R_2 / \Delta R / R_0$

Energy Resolution:

$\Delta(T)\ /\ (T) \sim \quad \Delta R / R_2$

Analyzer Constant:

For $V_0 = V / 2$: $R_0 = 2\,R_1 R_2\ /\ (R_1 + R_2)$**, i.e.**

$T \quad = \quad k\,q\,V_0,$

$\mathbf{k} = (R_1 + R_2)\ /\ 2\,\Delta R\ =\ R_c / \Delta R$

The **Analyzer Constant k** depends only on the Geometry. The constant **k** determines the ratio of Energy/charge and the voltage on the analyzer plates.

Conditions for Transmission, II. General Case ($\alpha \neq 0$):

$T_\infty = T(r) + q\,\phi\,(r) = T(r) - q\,K / r + q\,\phi_\infty,$

Particle trajectories in the analyzer are ellipses with major axis a

$a \quad = \quad -\,q\,K / 2\,E,$ with

$E \quad = \quad T(r) - q\,K / r$

Transmission:

$TR = \langle d\alpha\ dv/v \rangle = 1/4\,(\Delta R / R_c)^2\ \csc^3(\Phi/2)\ \ (7/8 + \cos(\Phi/2))$

(e.g. $\Phi = 90°$: Quadrispherical Analyzer)

(Ref.: e.g. Paolini and Theodoridis, 1967; Gosling et al., 1978)

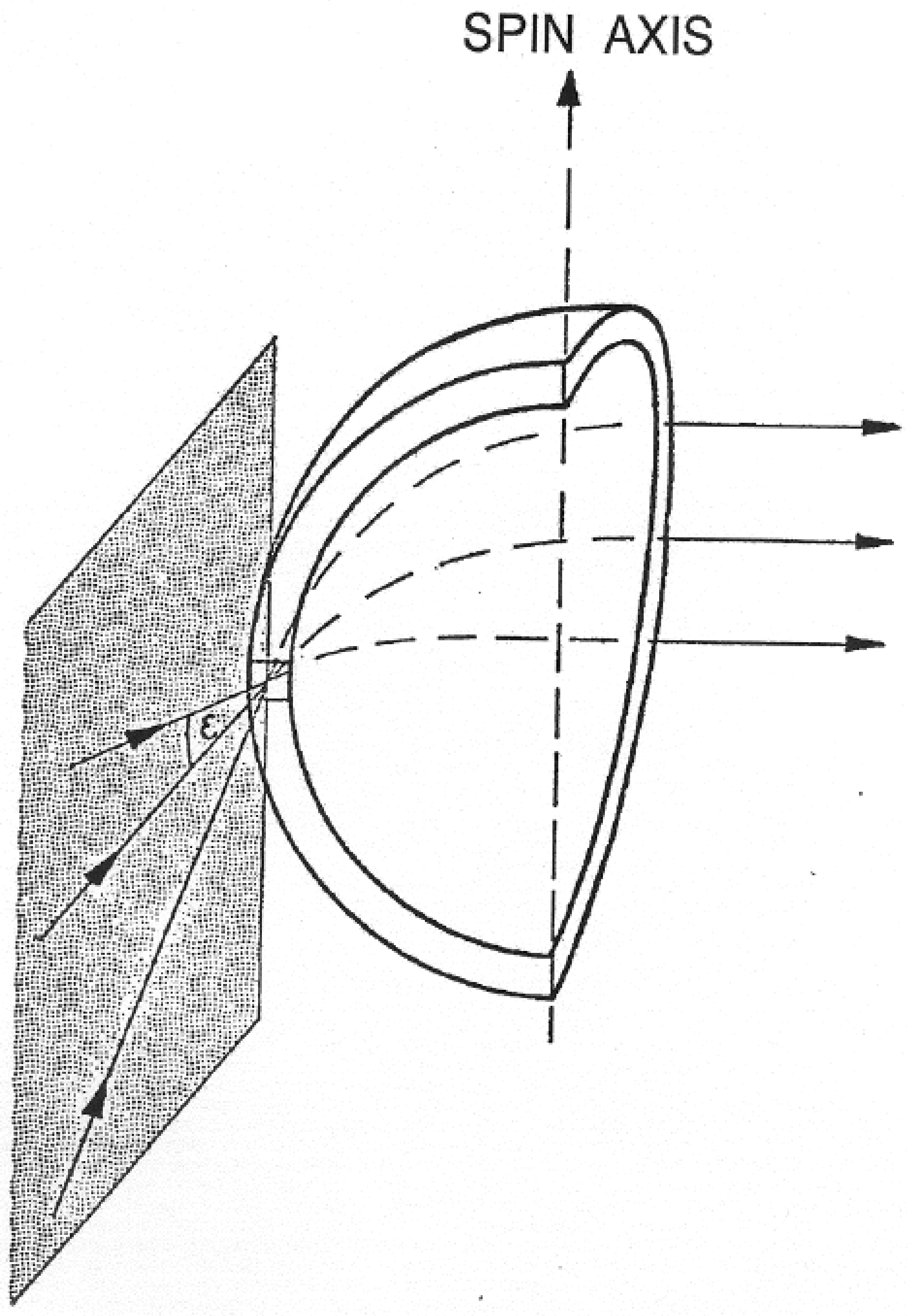

SPIN AXIS
ε

THE NEXT STEP: 3D RESOLUTION IN 1 SPIN

A SYMMETRICAL QUADRISHERICAL ANALYZER IN TOP HAT CONFIGURATION

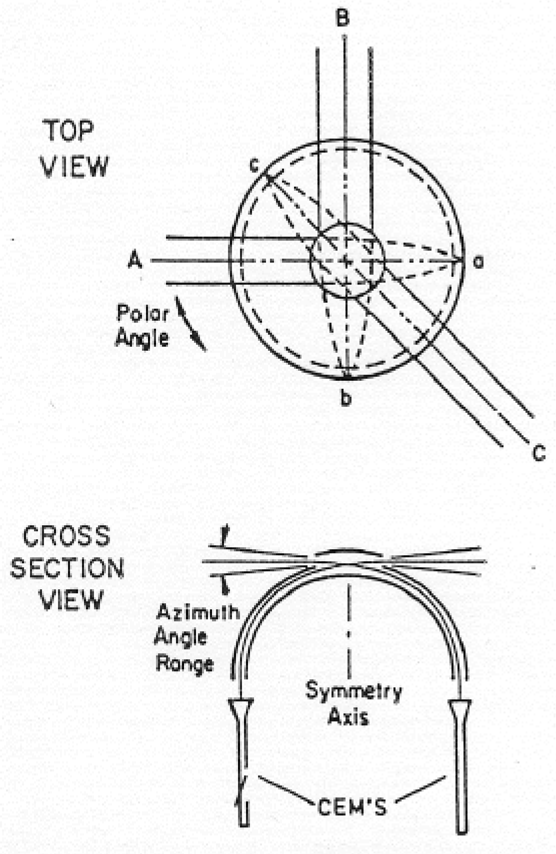

Fig. 1. The basic geometry and angular response of a symmetrical quadrisphere. The top figure illustrates why the analyzer, in principle, has a uniform response over 360° of polar angle. In the AMPTE application, only 180° are actually utilized.

AMPTE / IRM Plasma Package

(Paschmann et al., 1985, Carlson et al., 1982)

MASS / CHARGE ANALYSIS

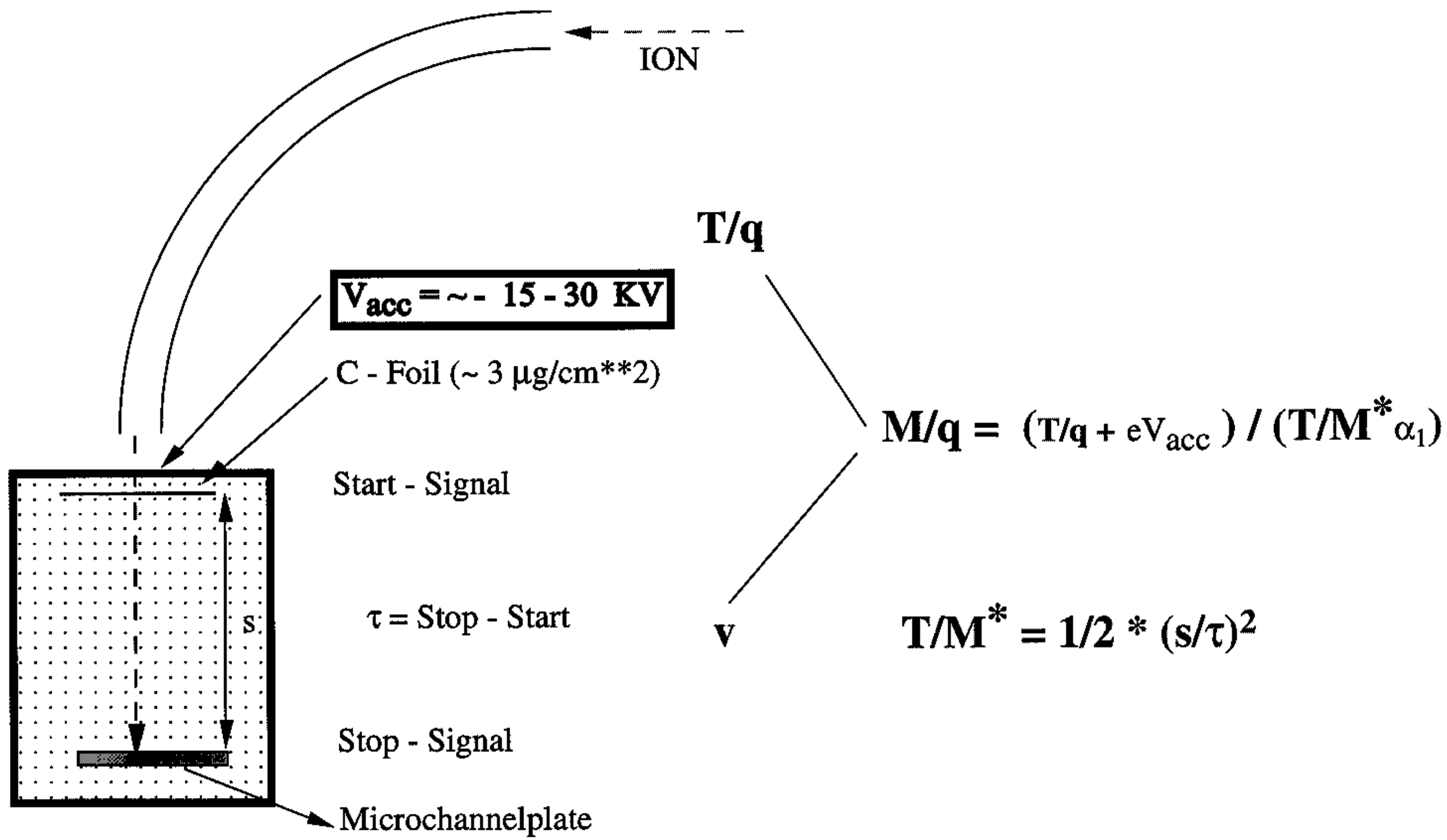

VELOCITY DETERMINATION

Determination of velocity by time-of-flight (TOF) measurement. Timing signal from **S**econdary **E**lectron **E**mission (SEE) from START and STOP sensor elements.

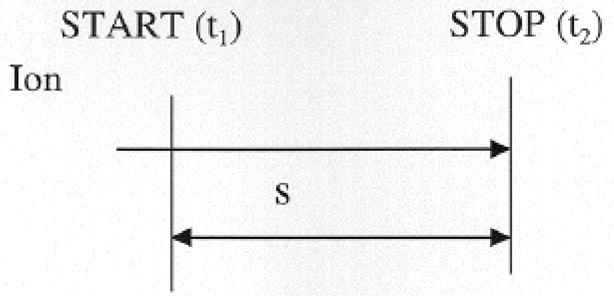

$\tau = t_2 - t_1$

$V = s / \tau$

Accuracy determined by:

- Path length variations (scattering)
- Energy variations in START element
- Variations of timing signal

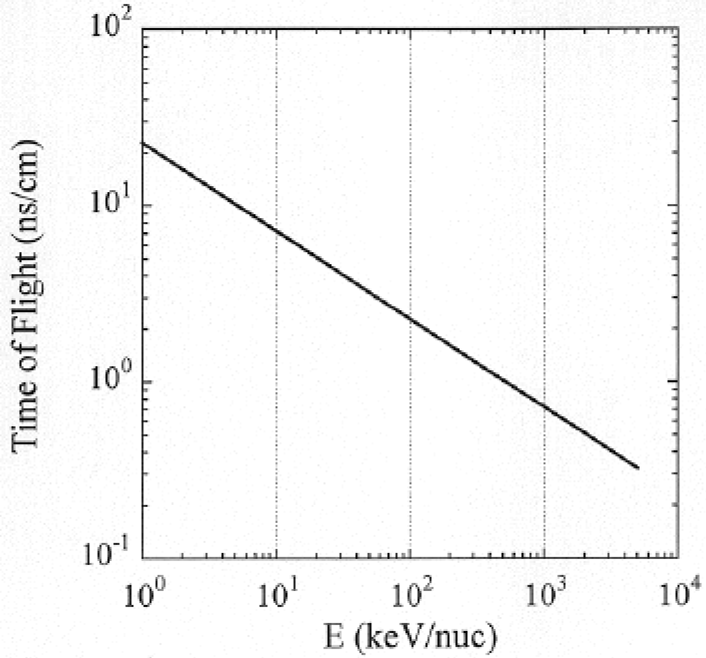

CODIF
The Ion Composition and Distribution Function Analyzer

for the Missions

CLUSTER-1

FAST

Equator-S

CLUSTER-2

in the Magnetosphere of the Earth

CIS-1 (CODIF)

Principles of Operation

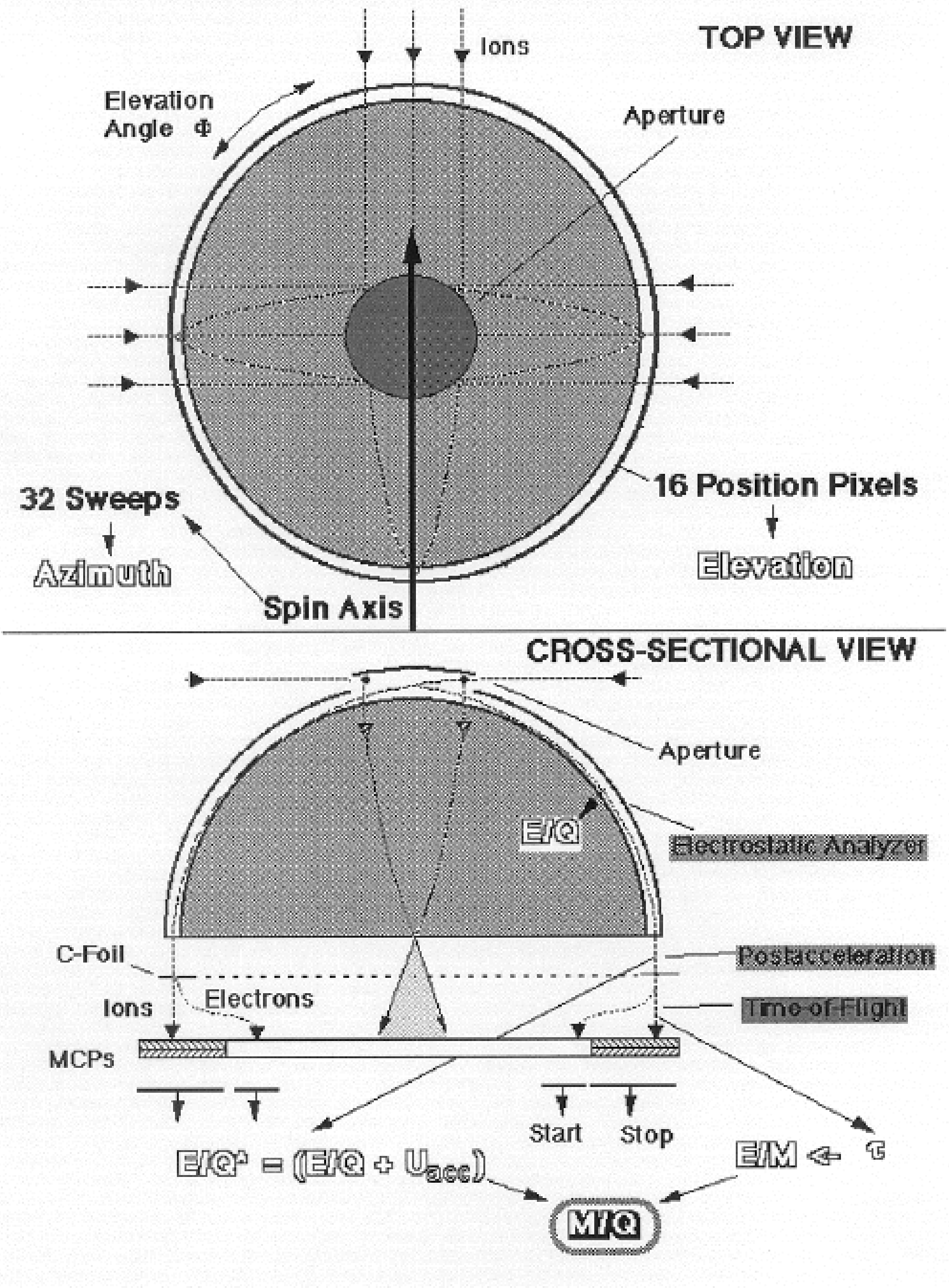

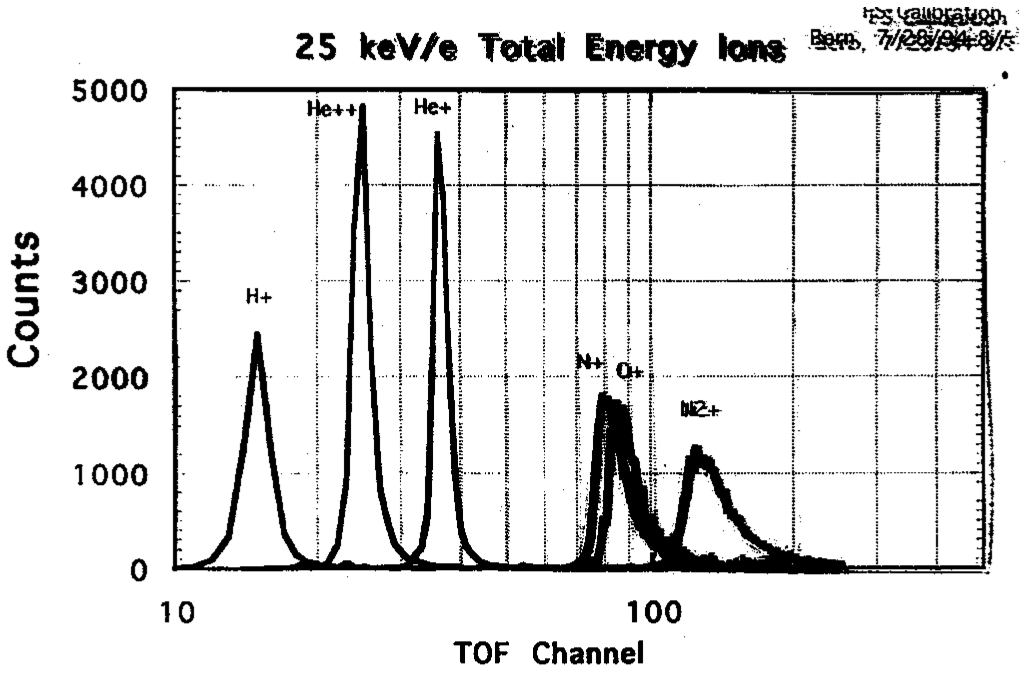

Figure 16. Time-of-flight spectrum of 25 keV H^+, He^{++}, He^+, N^+, O^+, and $N_2{}^+$ ions, as mea with the Flight Spare model of CODIF during a calibration at the University of Bern.

High Resolution Mass Determination:
THE LINEAR ELECTRIC FIELD ANALYZER

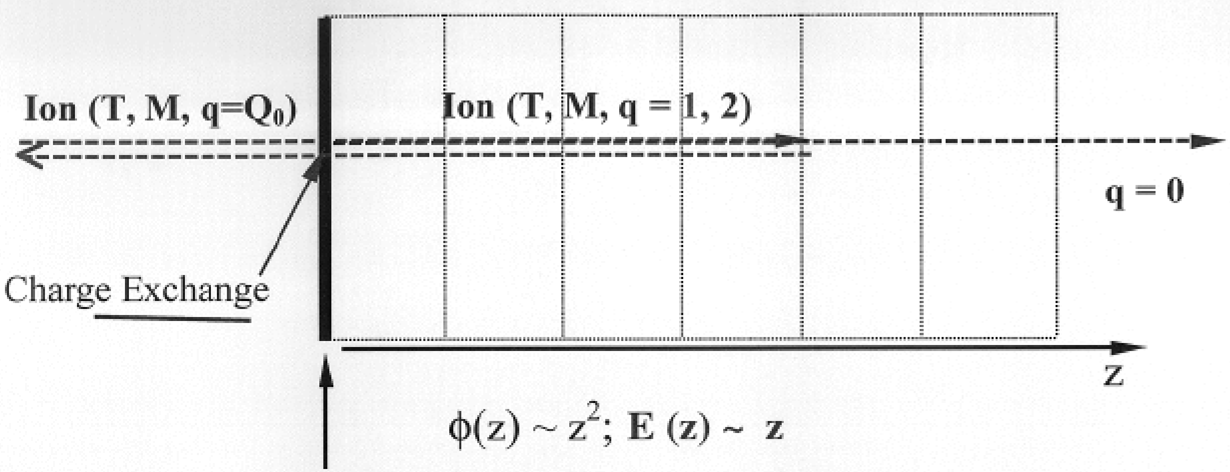

$\phi(z) \sim z^2$; **E (z) ~ z**

Dominant charge state of **Ions** at low energies (keV/nuc): **q = 1**

E = - k z **C- Foil**

$M\, dz^2 / dt^2 = -q\, k\, z$

Solution: Harmonic Oscillator

$z(t) = A \sin(\omega t + B)$; with $\omega = \sqrt{(k\, q / M)}$, and (for 1/2 oscillation)

$\tau = \pi \sqrt{(M / q\, k)}$, independent of particle energy and trajectory.

High Mass Resolution: $M/\Delta M \sim 100$!

OPERATIONAL IN SPACE:

WIND (Gloeckler et al., 1995)
SOHO (Hovestadt et al., 1995
ACE (Gloeckler et al., 1998)
CASSINI (Young et al., 1997)

Ref.: Managadze, 1986; Yoshida, 1986; Hamilton et al., 1990; Möbius et al., 1990; Wurz et al., 1997

DEMONSTRATION OF THE MASS RESOLUTION OF A LINEAR ELECTRIC FIELD (LEF) ANALYZER

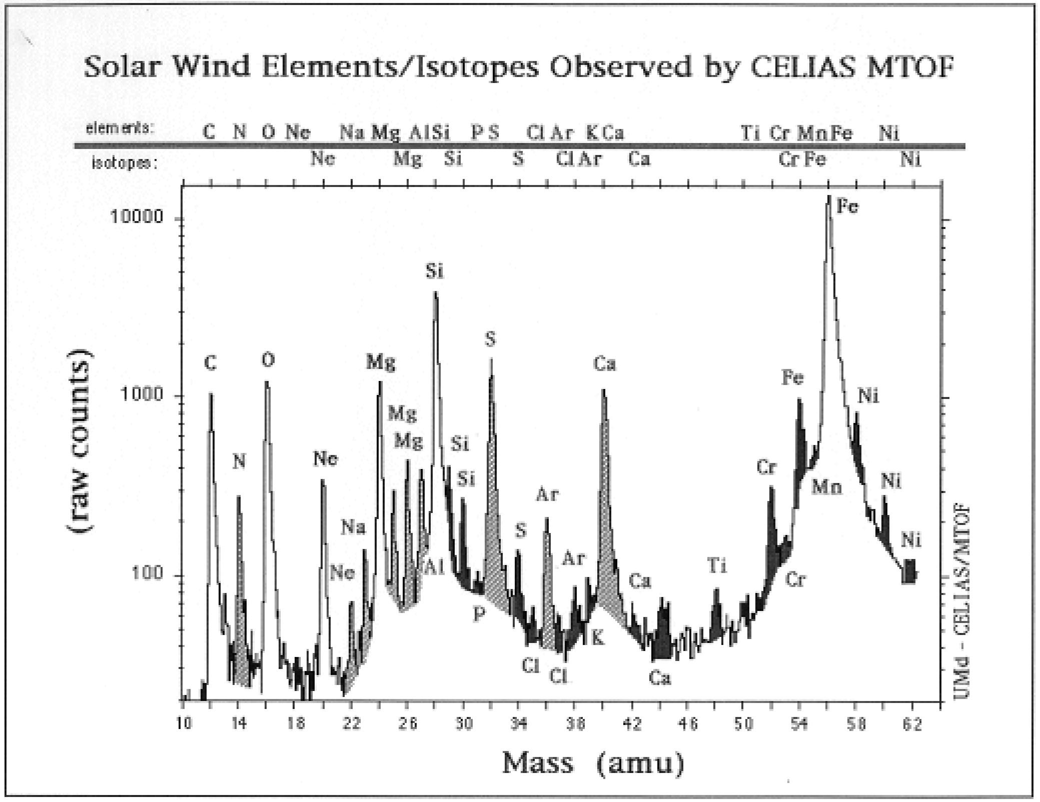

Solar Wind Data (3 day average), MTOF / CELIAS / SOHO Public Information Page, Ipavich et al., 1996

THE CASSINI PLASMA SPECTROMETER INVESTIGATION (CAPS)

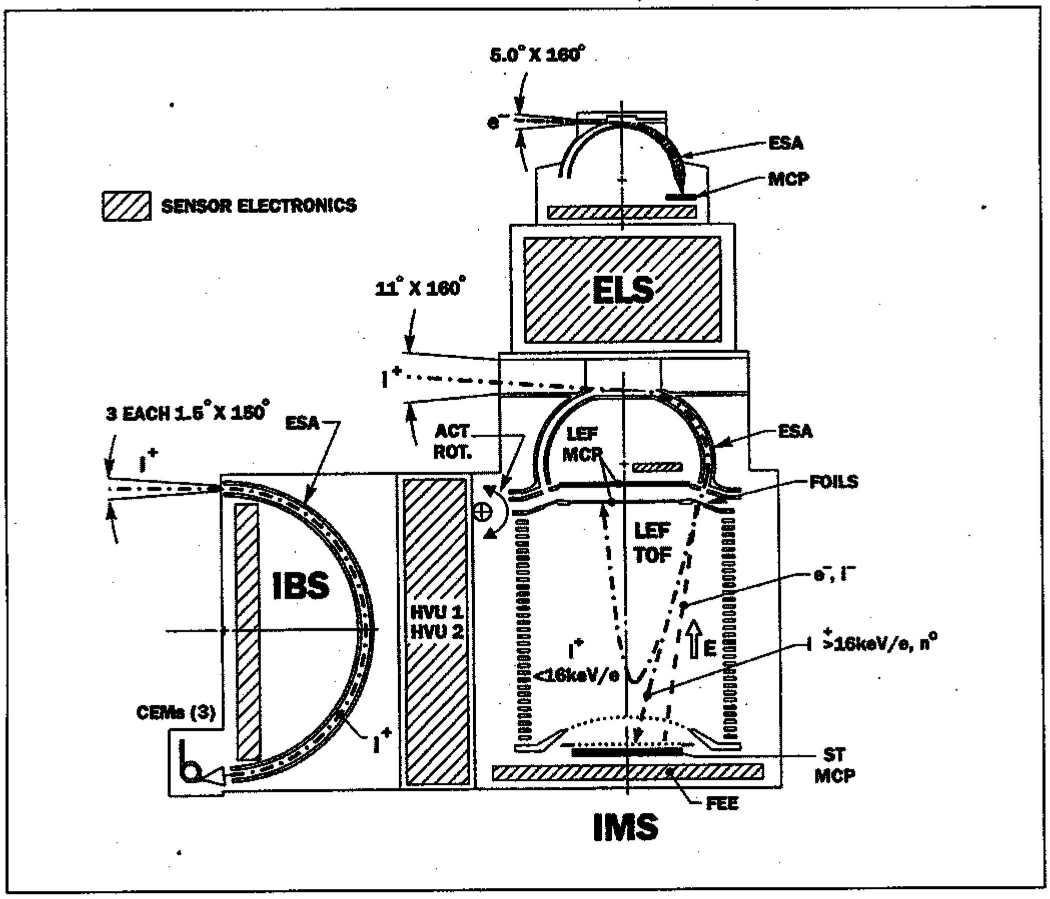

	ELS	IMS
Energy Range:	1 – 30000 eV	1 – 50000 eV/q
Mass/charge		
Range	-	1 – 60
Resolution (M/ΔM):	-	50 (<16 keV/e)
		8 (>16 keV/e)

Mass: 23.2 kg

Power: 16.4 W

MASS / CHARGE AND MASS ANALYSIS

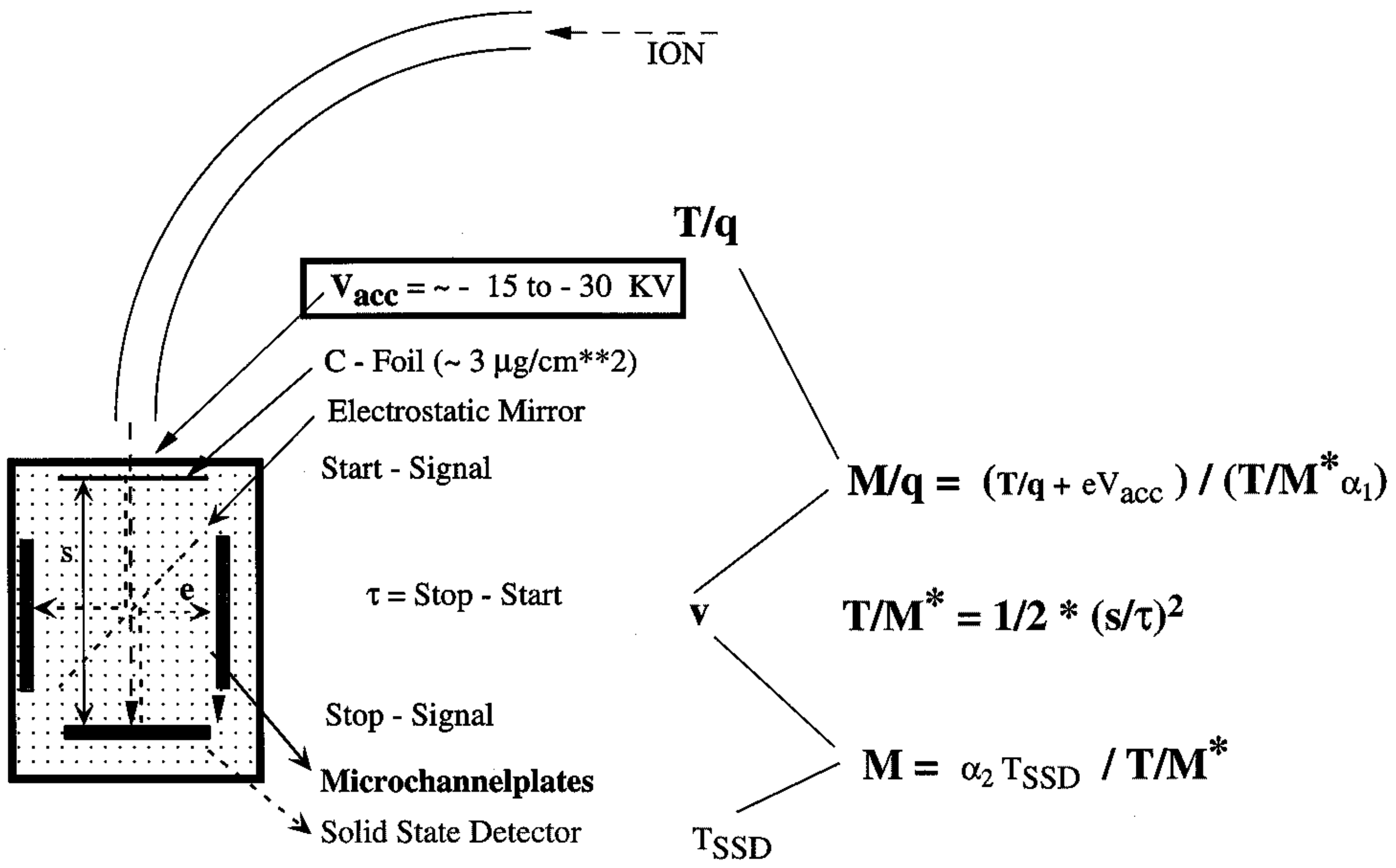

ENERGY DETERMINATION

Energy Measurement

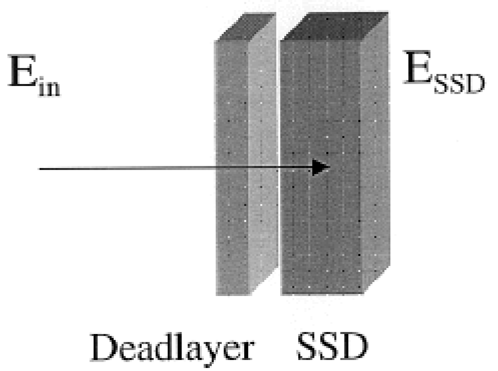

$$E_{SSD} = E_{in} - \Delta E_{deadlayer} - \Delta E_{NC}$$

E_{SSD}	Measured Energy
$\Delta E_{deadlayer}$	Energy loss in inactive SSD surface layer, front foil, etc.
ΔE_{NC}	Non-electronic energy loss (nuclear collisions)

ENERGY and POSITION Determination:

Use of 'Stripe'-Detectors or of 'Pixel' Detektors

THE CHARGE-ENERGY-MASS SPECTROMETER for 0.3-300 keV/e IONS ON THE AMPTE / CCE SPACECRAFT

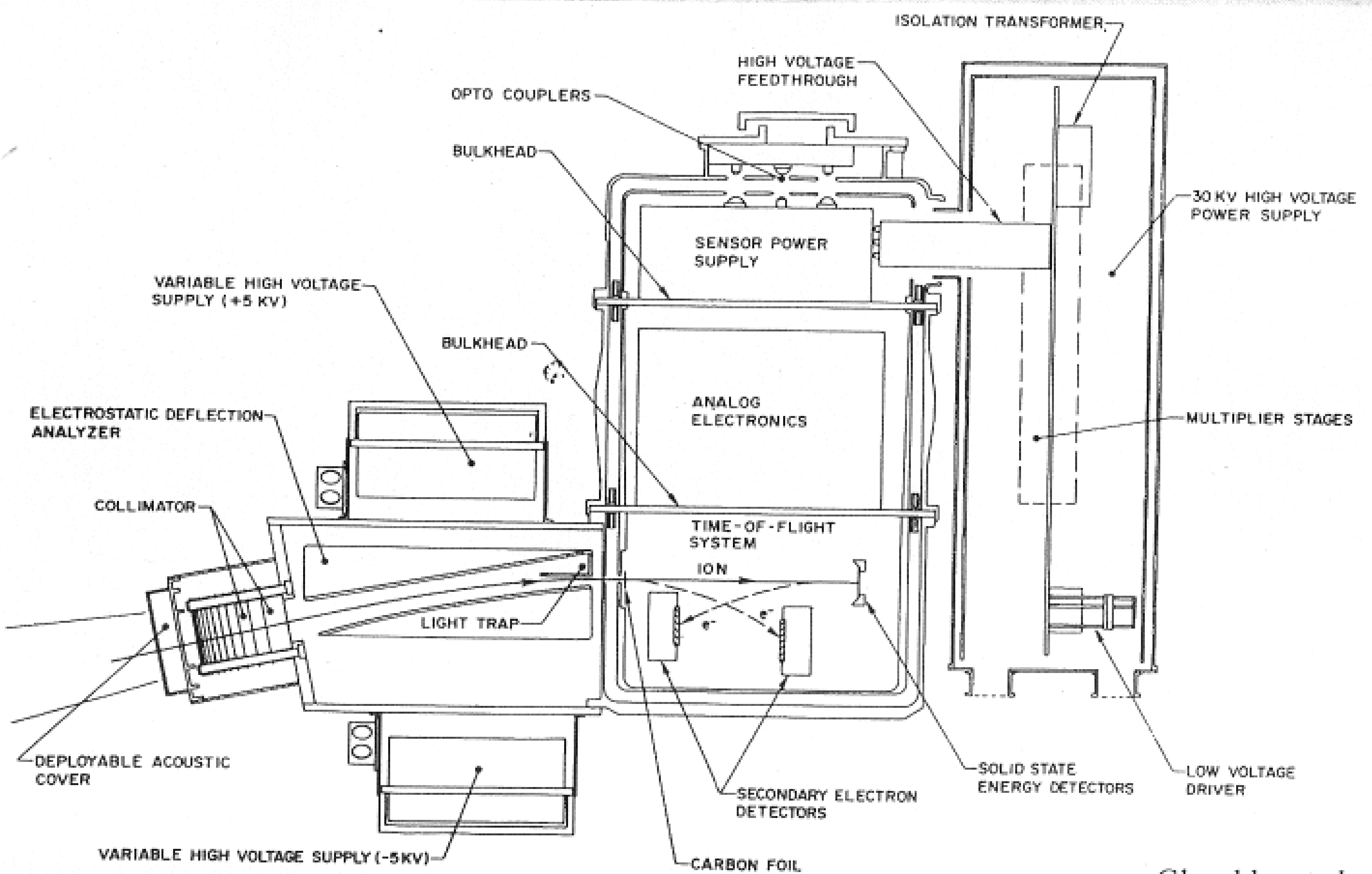

Gloeckler et al., 1985

SENSOR SYSTEMS FOR HIGHER ENERGIES

DETERMINATION OF ENERGY AND MASS (OR Z)

(1) TOF - E Determination

Improvements on the upper energy limit of the TOF measurements by

- Improving the resolution of the TOF measurement
- Increasing the length of the TOF-path
- Using passive collimator –> ***No Ionic Charge Measurement***

(2) dE/dx – E and Range –E Particle Telescopes

- Advantage: Higher maximum energy
- Disadvantage: Minimum energy limited by ΔE Element(s)

(3) Hybrid Sensors, using both, TOF and dE/dx Techniques

ENERGY AND MASS ANALYSIS

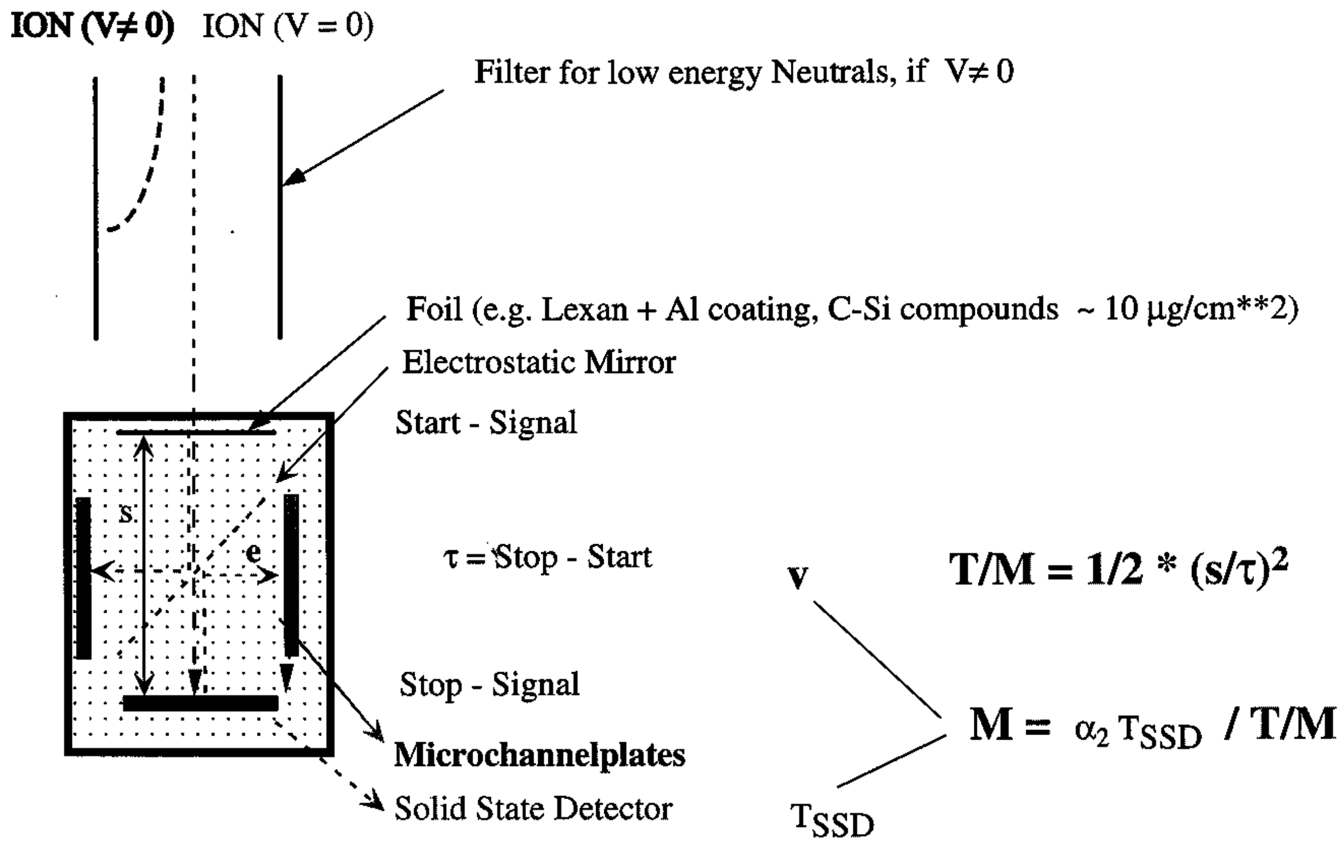

$$T/M = 1/2 * (s/\tau)^2$$

$$M = \alpha_2 T_{SSD} \; / \; T/M$$

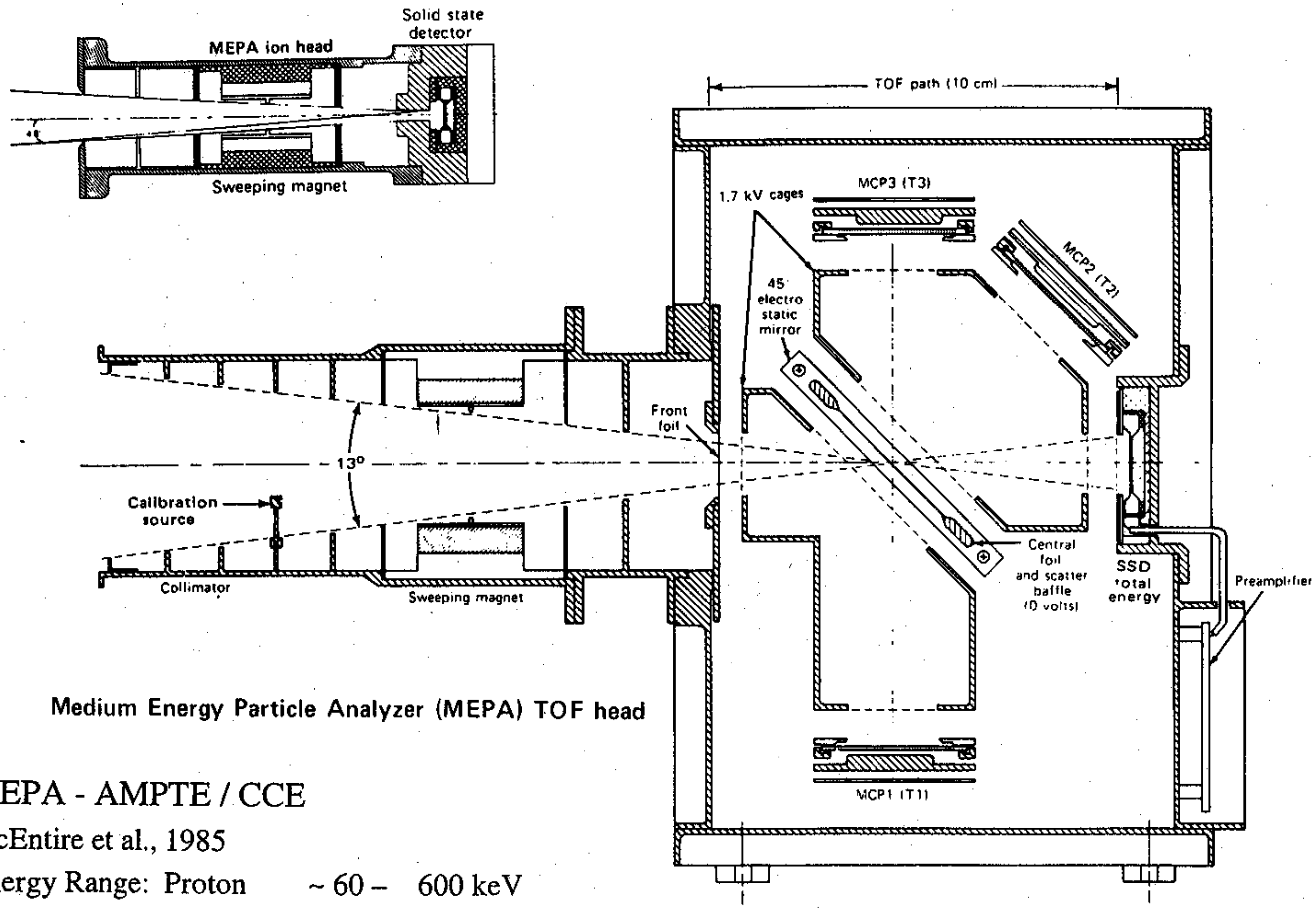

Medium Energy Particle Analyzer (MEPA) TOF head

MEPA - AMPTE / CCE

McEntire et al., 1985

Energy Range:	Proton	~ 60 – 600 keV
	He	~ 79 – 1900 keV
	Fe	~900 – 1400 keV

Fig. 1. Cross-sectional views of the (a) MEPA TOF head and (b) ion head. Ions incident on the TOF head pass through the front and central foils and stop in the rear SSD. Secondary electrons from the surface of the front foil and SSD are accelerated into the 1.7-kV electrostatic cages, reflected at the central electrostatic mirror, and image onto MCP1 and MCP3, respectively. Electrons emitted from the central foil are accelerated directly onto MCP2.

RESEARCH WITH ADAPTIVE PARTICLE IMAGING (RAPID) ON CLUSTER-2

IMAGING ION MASS SPECTROMETER (IIMS)

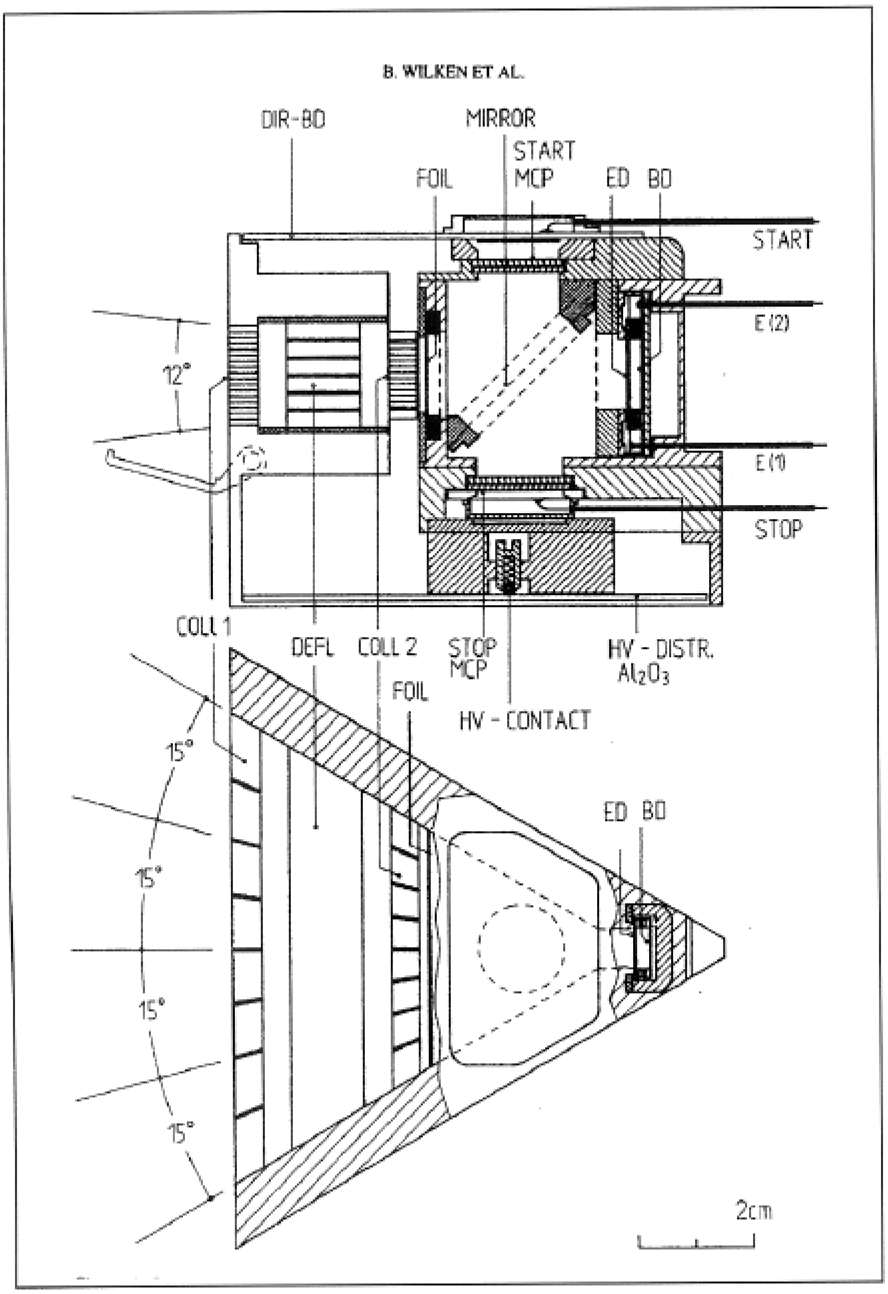

IIMS SENSOR CHARACTERISTICS

Flightpath:	34 mm
Field of view:	6° x 60°
Polar Angle:	4 x 15°
Energy-SSD:	5 x 15 mm^2 / 300 µ
Anticoincidence-SSD:	5 x 15 mm^2 / 300 µ

Energy Range

H	(-, t)	40 – 75	keV
	(E, t)	75 – 1500	keV
He	(-, t)	40 – 75	keV
	(E, t)	100 – 1500	keV
CNO		210 – 1500	keV
ENA		40 – 200	keV

Geometric Factor: 0.027 cm^2 sr

Wilken et al., 1997

SENSOR SYSTEMS FOR HIGHER ENERGIES

DETERMINATION OF ENERGY AND MASS (OR Z)

(2) PARTICLE dE/dx-E and Range-E TELESCOPES

The dE/dx – E Method

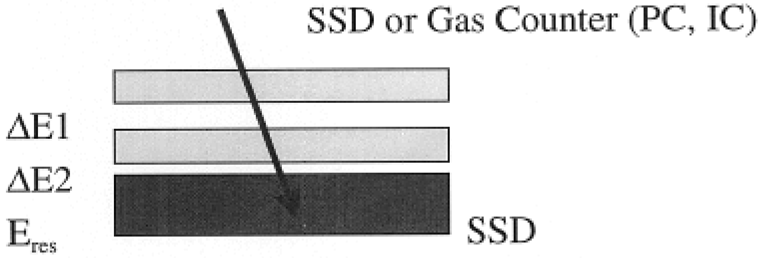

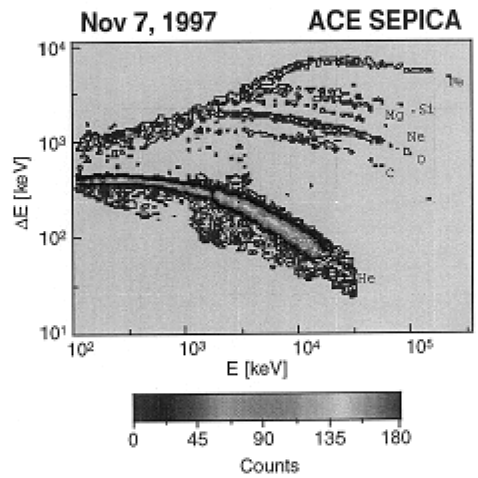

The measurement of Energy Loss (dE/dx), Range, and Residual Energy (E_{res}) of ions and electrons can be used to determine the total energy E, Nuclear Charge, and Mass.

For Ions:

$$dE/dx = k1 * Z^{*2} / (E/A) * f(k2,E)$$

PROTON – ELECTRON TELESCOPE (PET)
SAMPEX

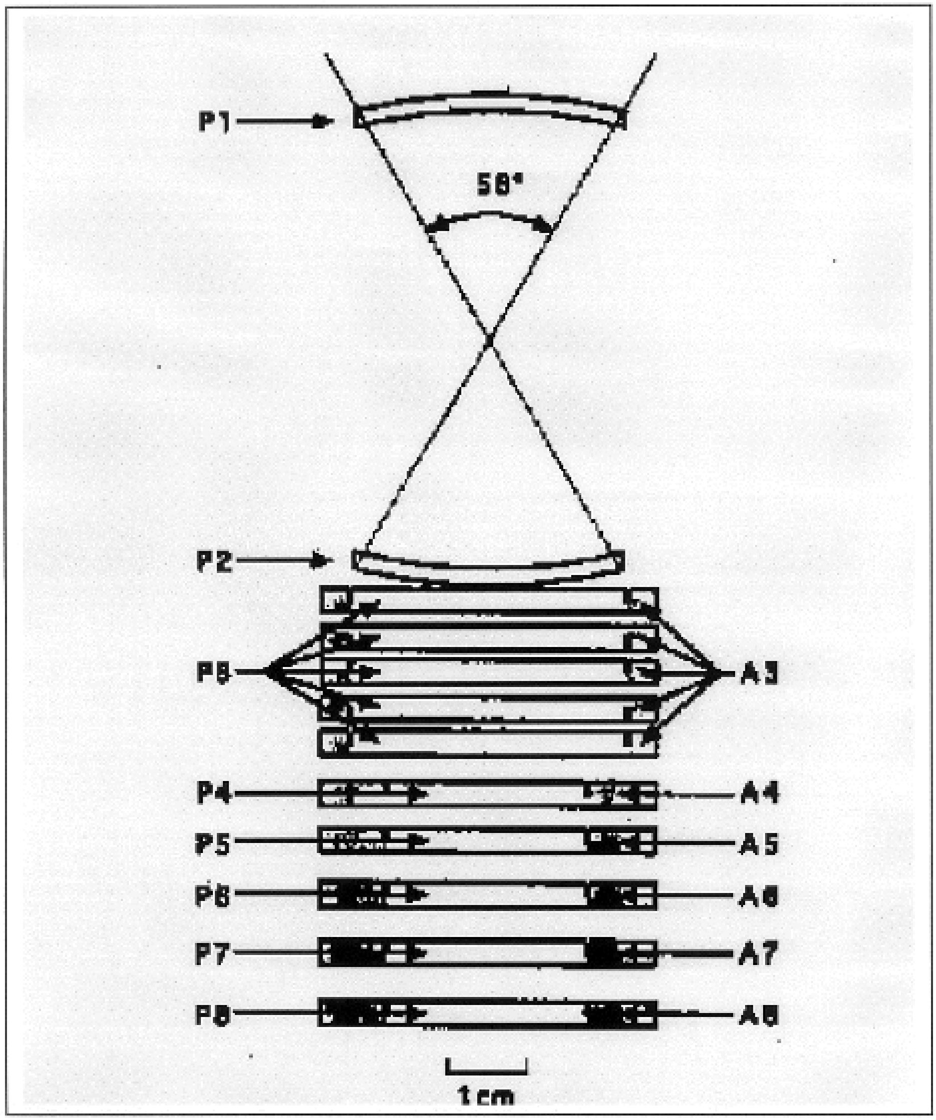

	p	e
Energy Range *	~ 19 - 85 MeV/nuc	0.4 – 30 MeV
Geometric Factor*	0.3 – 1.8 cm^2 sr	0.3 – 1.8 cm^2 sr

(*) for coincidence measurement

Cook et al., 1993

Long-Term Measurements of Highly Relativistic Electrons in the Magnetosphere

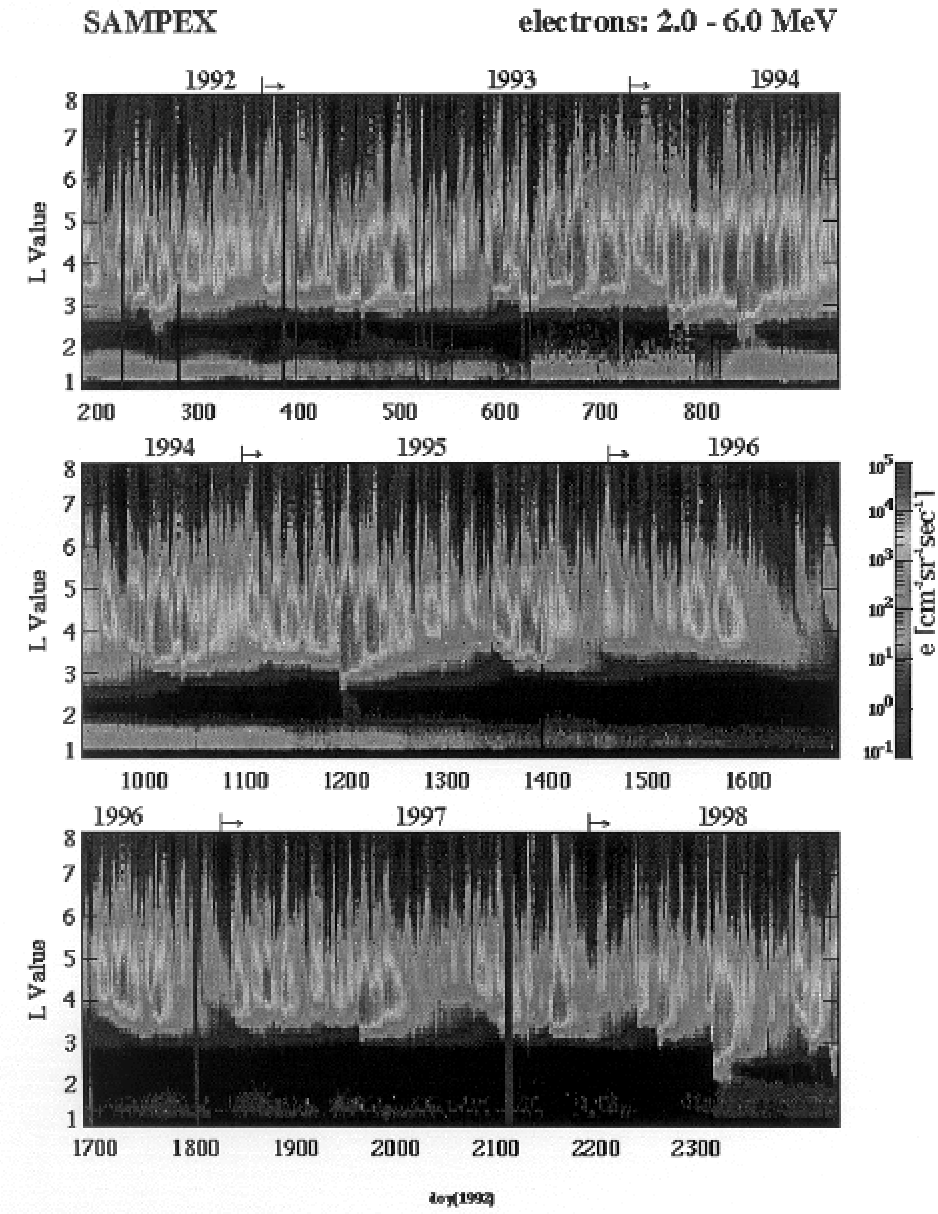

(from SAMPEX Science / WWW Page; contributed by Dan Baker, LASP, U of Colorado)

HIGH SENSITIVITY TELESCOPE (HIST)
CEPPAD / POLAR

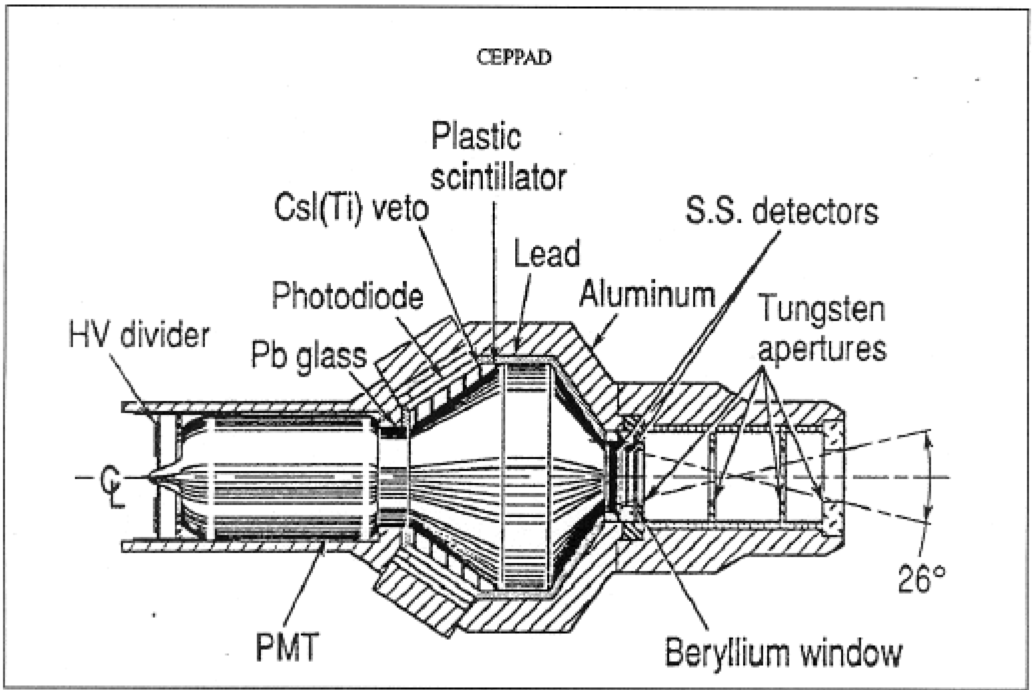

Proton / Electron Telescope

SSDs

SSD 1 (ΔE): 300 μm; SSD 2 (E_{res}): 2 mm

	p	e
Energy Range (MeV)	3.25 – 80	0.35 – 10
Nr. of Energy Bins	16	16
Field of View (conical)	26°	26°
Geometrical Factor (cm^2 sr)	0.088	0.088

Blake et al., 1995

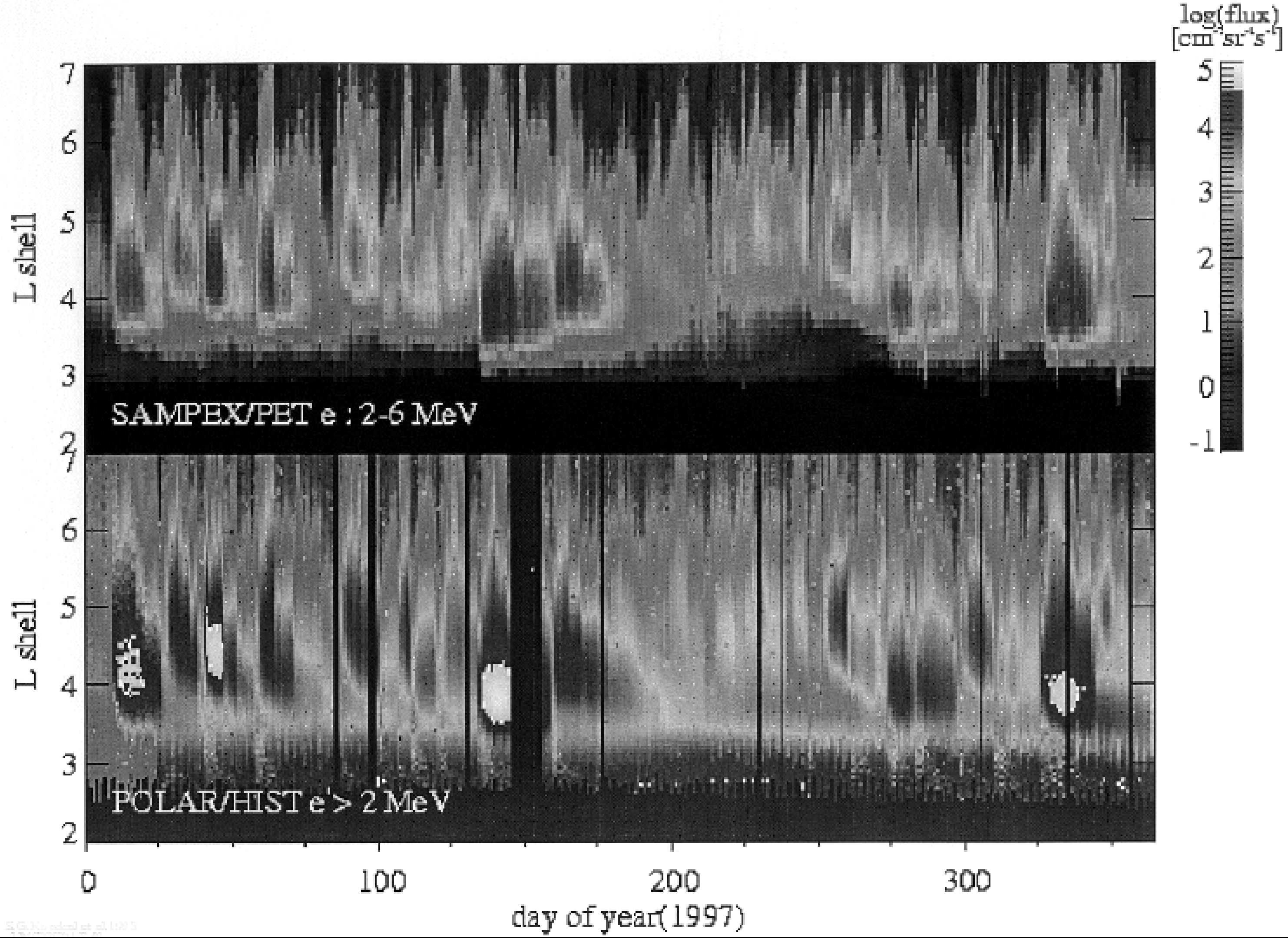
log(flux)
[cm⁻²sr⁻¹s⁻¹]
SAMPEX/PET e : 2-6 MeV
POLAR/HIST e > 2 MeV
L shell
L shell
day of year(1997)
0
100
200
300
7
6
5
4
3
2
5
4
3
2
1
0
-1

CUTOFF VARIATION DURING SEP EVENTS

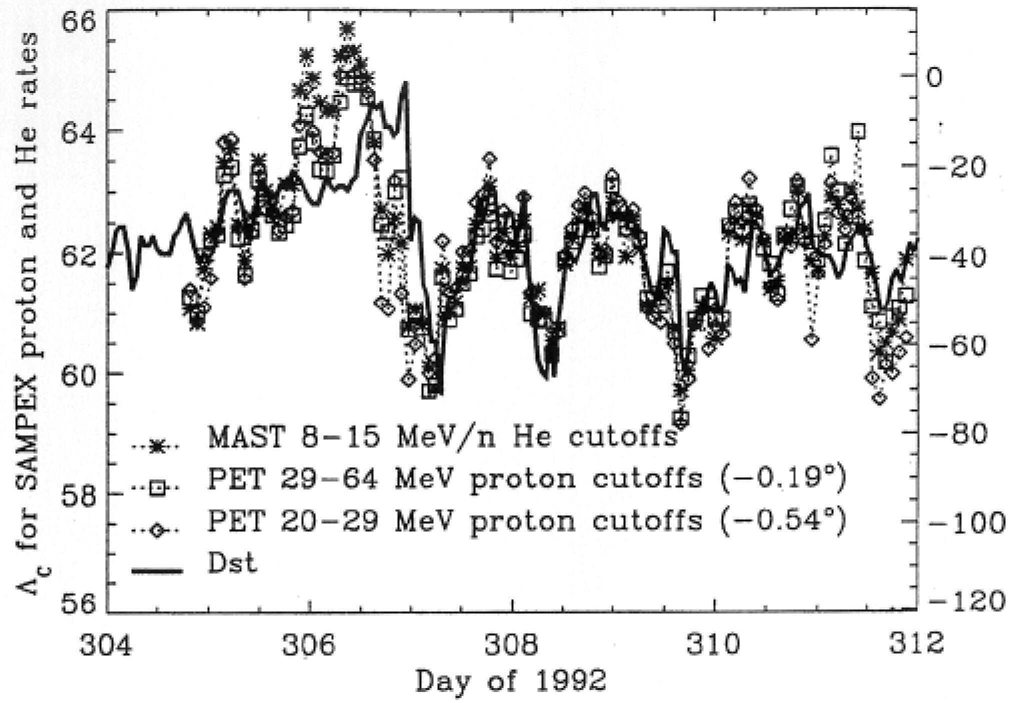

The orbit-averaged cutoff invariant latitude as determined from 3 SAMPEX p and ^{4}He rates, plotted versus time, and compared with Dst. The large variations of the Cutoff during active time periods (SEP events) could have a significant influence on the total dose at mid latitudes in Low Earth Orbit, e.g. at the ISS orbit (Leske et al., ICRC 2, p 381, 1997).

Correlation of Relativistic Electrons in the Magnetosphere with Solar Wind Parameters

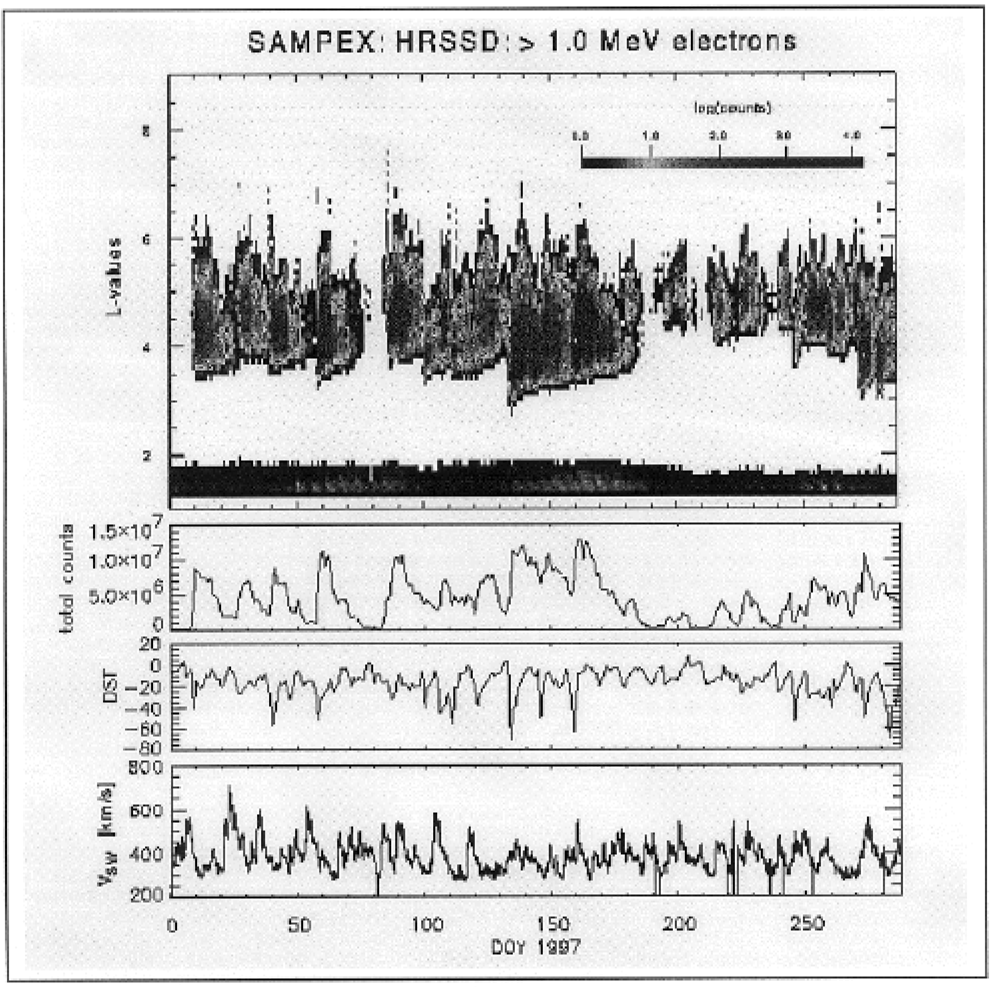

Kucharek et al., 2000

REMOTE SENSING OBSERVATIONS

GROUND OBSERVATIONS

European Incoherent SCATter Radar (EISCAT)

Measured Quantity:

- Echo of radar signal, scattered by ionospheric electrons

Inferred Quantity

Ionospheric Plasma Parameters

- Electron Density, Temperature
- Ion Temperature, Velocity, Composition

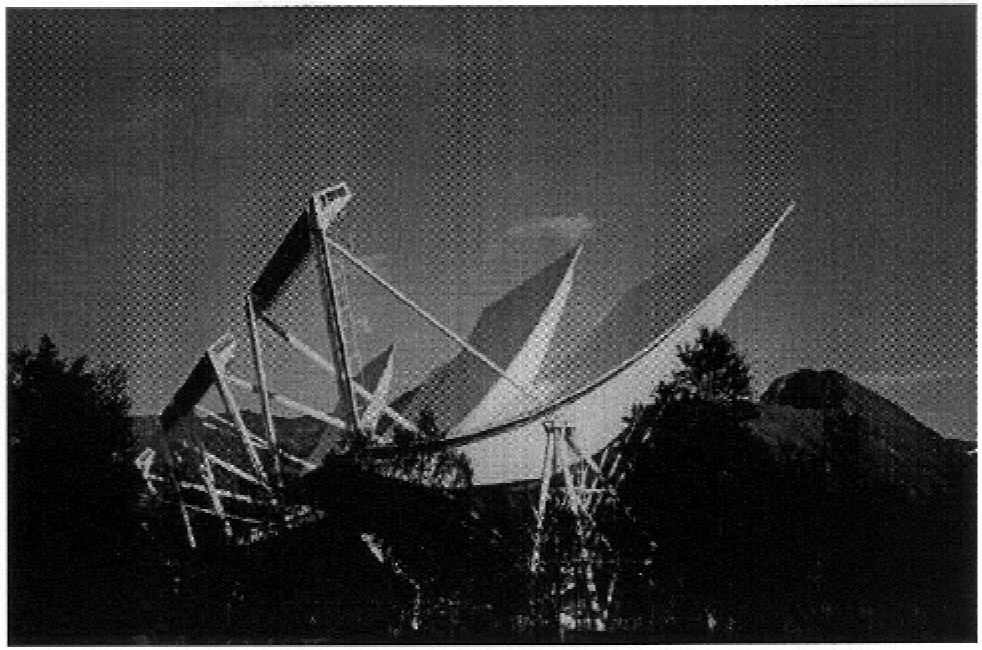

EISCAT: VHF Antenna

REMOTE SENSING OBSERVATIONS

IMAGING WITH VISIBLE LIGHT, UV, X-RAYS

(e.g. DE, POLAR, IMAGE)

Images of the aurora, recorded by the Polar Visible Imaging System and Ultraviolet Imager (two upper images on right) capture the global response of the geospace environment.

Geophysical Research Letters - Vol. 25, No. 14, 1998

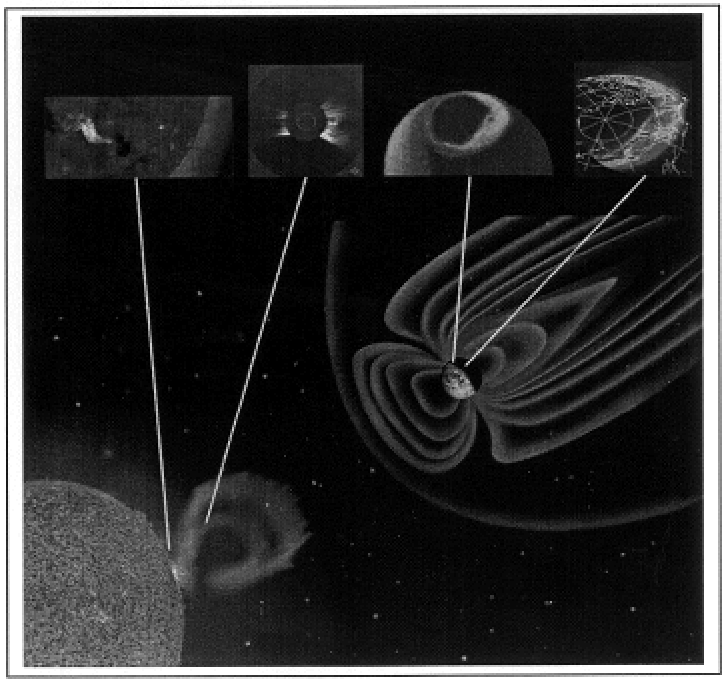

POLAR

Experiments: VIS, UVI, PIXIE

Energy input into the polar regions of the earth

Measured Quantity (e.g. Pixie):

3 – 60 keV X-rays from bremsstrahlung X-ray emission

Inferred Quantity:

Morphology, energy spectra, time variation of precipitating electrons

NEUTRAL PARTICLE IMAGING

Missions:

e.g. POLAR, IMAGE, CASSINI

Measured Quantity:

Energetic Neutral Atoms (ENA) from charge exchange of energetic ions with the neutral H exosphere

Inferred Quantity:

Distribution, energy spectra, and time variation of energetic ions

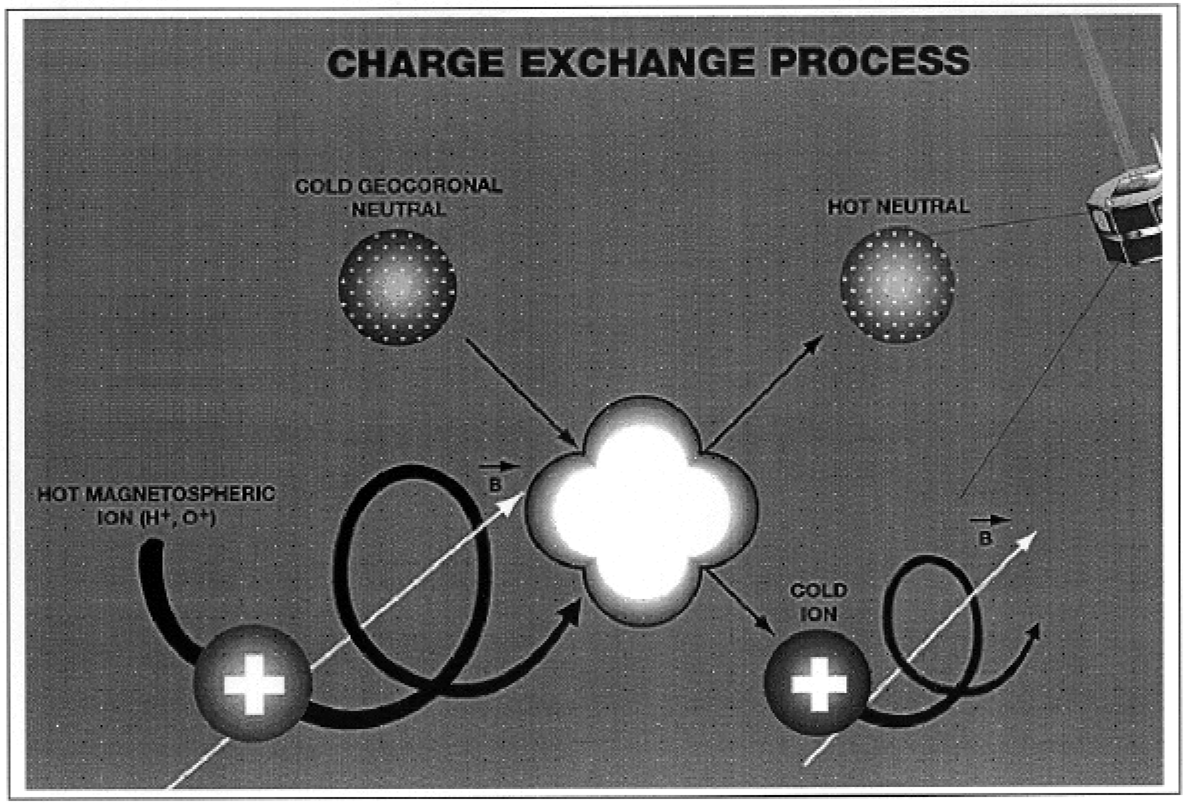

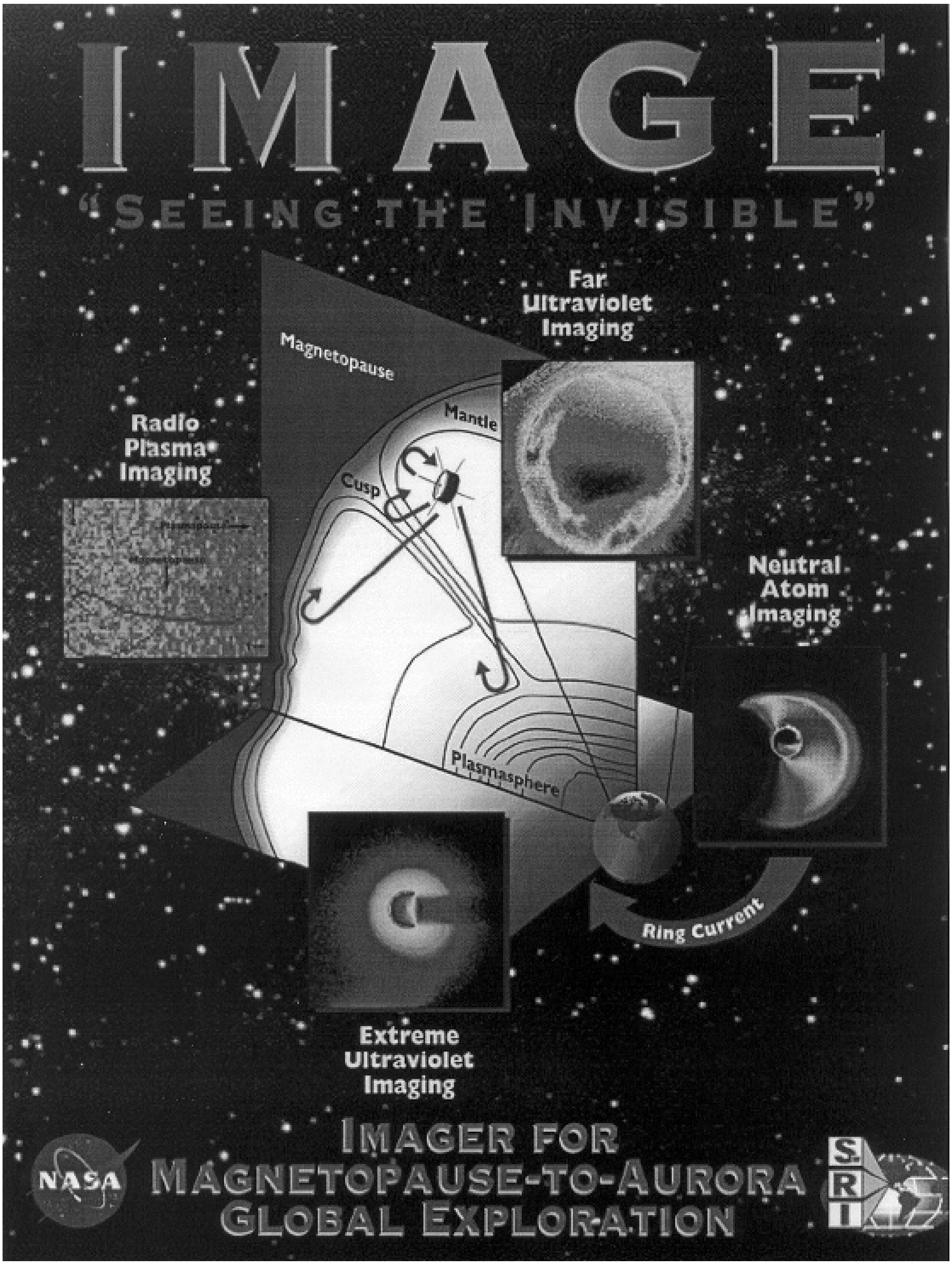
IMAGE
"SEEING THE INVISIBLE"
Far Ultraviolet Imaging
Magnetopause
Radio Plasma Imaging
Mantle
Cusp
Neutral Atom Imaging
Plasmasphere
Ring Current
Extreme Ultraviolet Imaging
IMAGER FOR MAGNETOPAUSE-TO-AURORA GLOBAL EXPLORATION
NASA
SRI

EXPERIMENTAL TECHNIQUES FOR THE MEASUREMENT OF ENAs

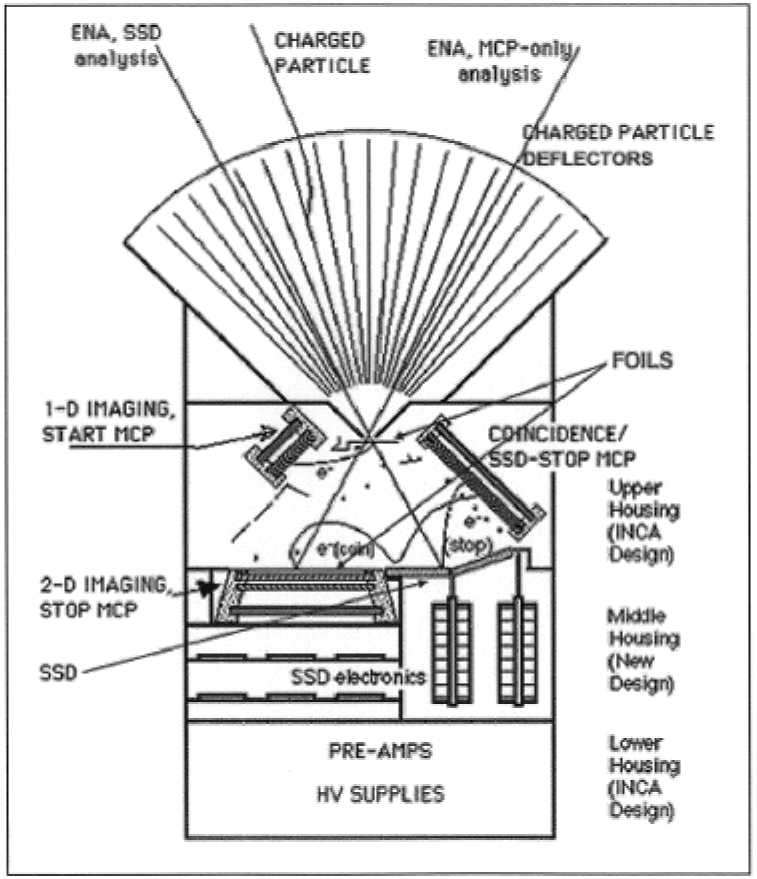

High-Energy Neutral Atom (HENA) Imager

Measurement Technique

- Discrimination against Ions by Electrostatic Deflection
- Position Measurement (1D, 2D) -> Trajectory
- TOF Measurement -> E / mass
- Energy Measurement -> E

Energy Range: 10 – 500 keV

Derived Quantities:

Neutral atom images of composition and energy of Ring Current and Near-Earth Plasma Sheet

Mitchell et al., Space Science Reviews, 91, 67-112, 2000

THE NEXT STEP: MULTISPACECRAFT MISSIONS

- Unfold Temporal and Spatial Variations in the Magnetosphere
- Explore Boundary Structures and Boundary Motions in Detail
- Provide a Dynamic Picture of the Magnetosphere and its Interaction with the Solar Wind
- Provide Global, 3D, Synoptic Images of the Magnetosphere

THE EXPERIMENTAL CHALLENGE

- Microsat and Nanosat Technology Development
- Development of Small Instruments (low mass and power) for Scientific Payload

MICROSATS AND NANOSATS

	Mission	Number of Spacecraft	Mass (kg)	Begin Phase C/D	Orbit	Technology Challenges
Near	Cluster II (ESA)	4	1180	'00 (launch)	4 x 20 R_e	
Near	Magnetospheric Multiscale	5	240	'04	Apogees from 12 to 127 R_e	Variable cluster
Near	Geospace Electrodynamic Connections	4	600	'05	130 x 2000 km	Dipping satellites
Near	Mag Constellation	100	10	'07	10-35 R_e	Dispenser ship, miniaturization
Mid	Inner Mag Constellation	42	10	'08- '14	2-12 R_e	Dispenser ship, radiation tolerance
Far	Dayside Boundary Constellation	39	10	'08- '14	2-20 R_e	Multiple inclination
Far	Solar Flotilla	12	50	'15- '25	Heliocentric (perihelion ~0.2 AU), various inclinations	Solar sails, deep-space microsats, near-solar communications
Far	Inner Heliospheric	12	50	'15- '25	Heliocentric (perihelion ~0.2 AU), various inclinations	Solar sails, deep-space microsats, near-solar communications
Far	Outer Heliospheric Radio Imager	16 (+ 1 mother ship)	25	'15- '25	20-40 AU	Interferometric RF measurements among 16 spacecraft; ~autonomous formation flying (~1000-km spacing) in deep space

CLUSTER-II

Status:

Launch 1 (S/C 2+3): 16 July 2000

Launch 2 (S/C 1+4): 9 Aug 2000

Orbit: 4 x 19.6 R_E

Commissioning / Test Phase in Progress (Aug - Dec 2000)

•

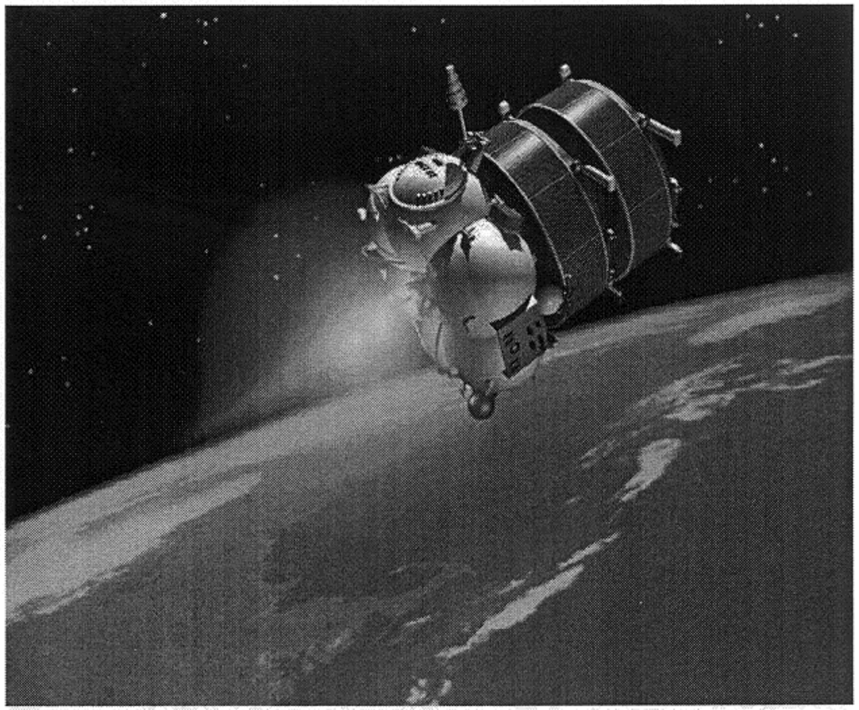

Fregat upper stage with two Cluster II satellites

CLUSTER ORBIT AND THE MAGNETOSPHERIC REGIONS OF INTEREST (SCHEMATIC)

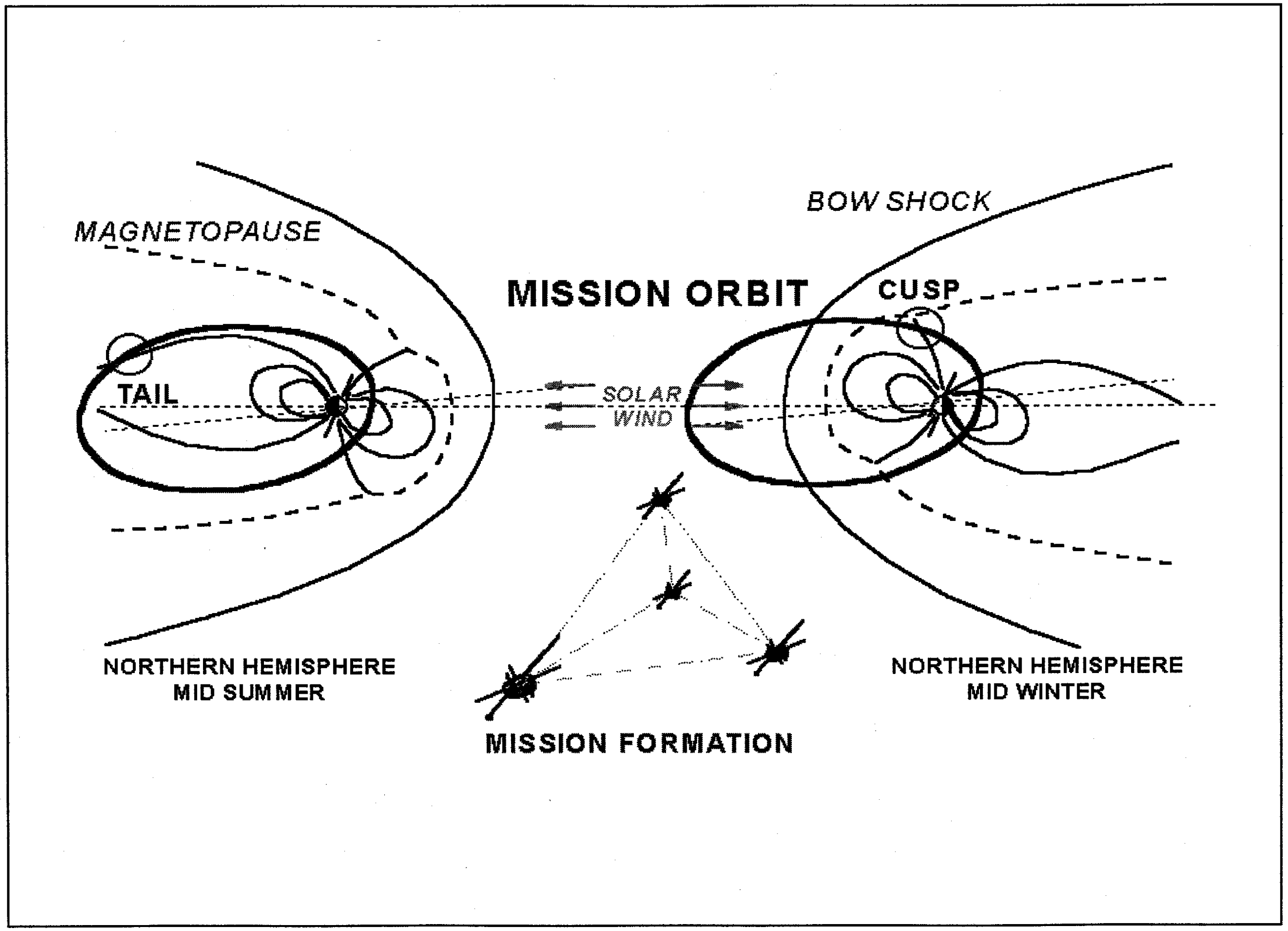

STORMS

Mission Proposal for next F2 / F3 Mission Selection in 2000 (ESA), Possible Launch Date: 2007

MISSION: 3 S/C in Equatorial Orbit

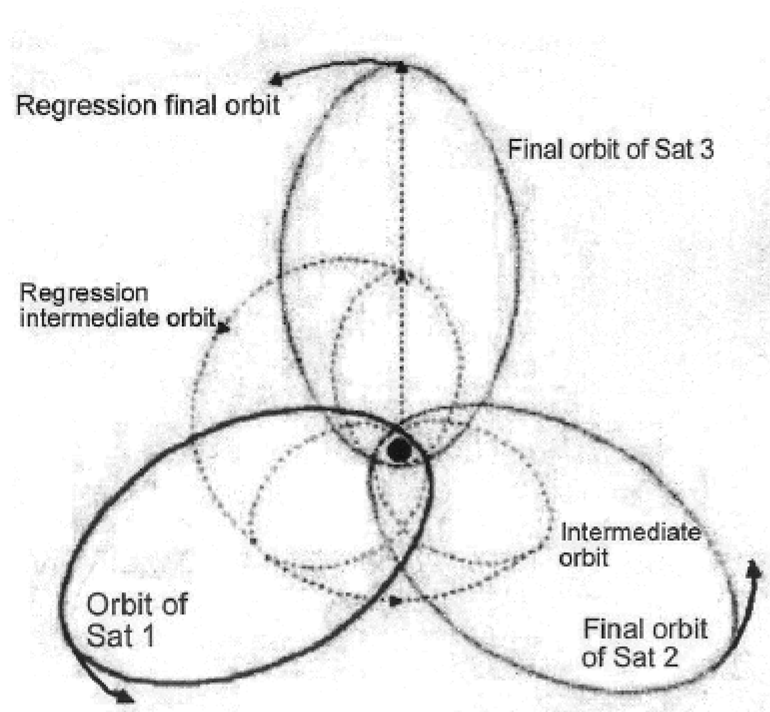

SPACECRAFT AND INSTRUMENTS

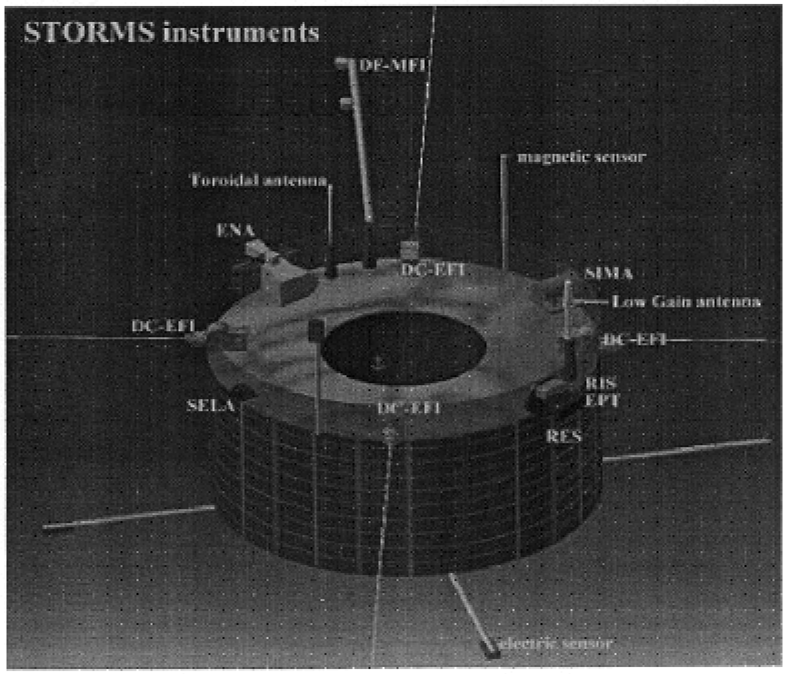

MAGNETOSPHERIC MULTISCALE MISSION (MMS)

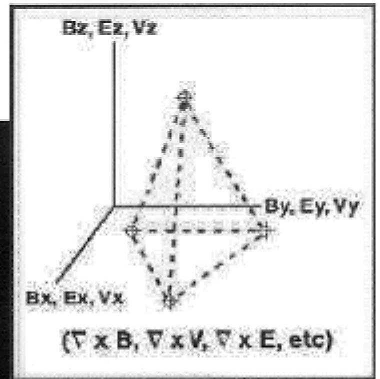

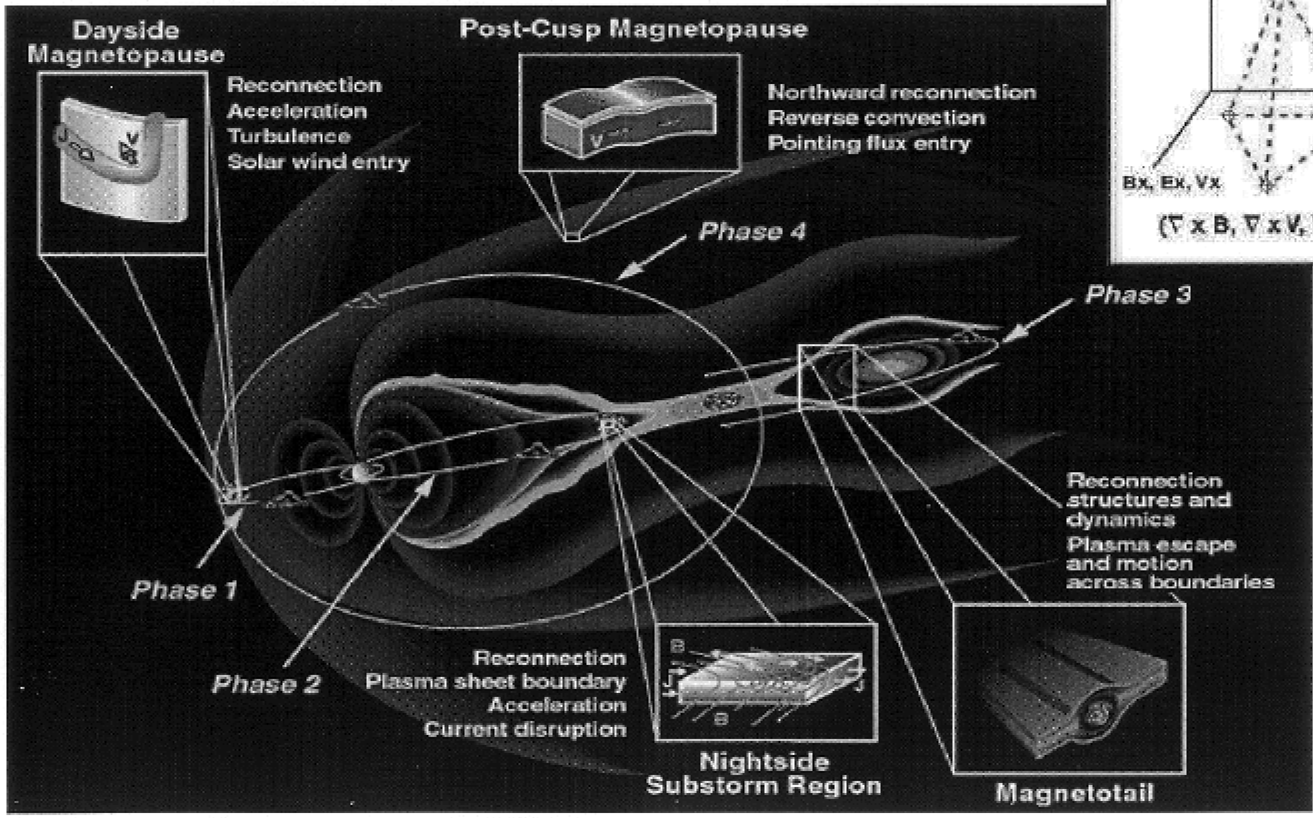

INNER MAGNETOSPHERE CONSTELLATION (IMS)

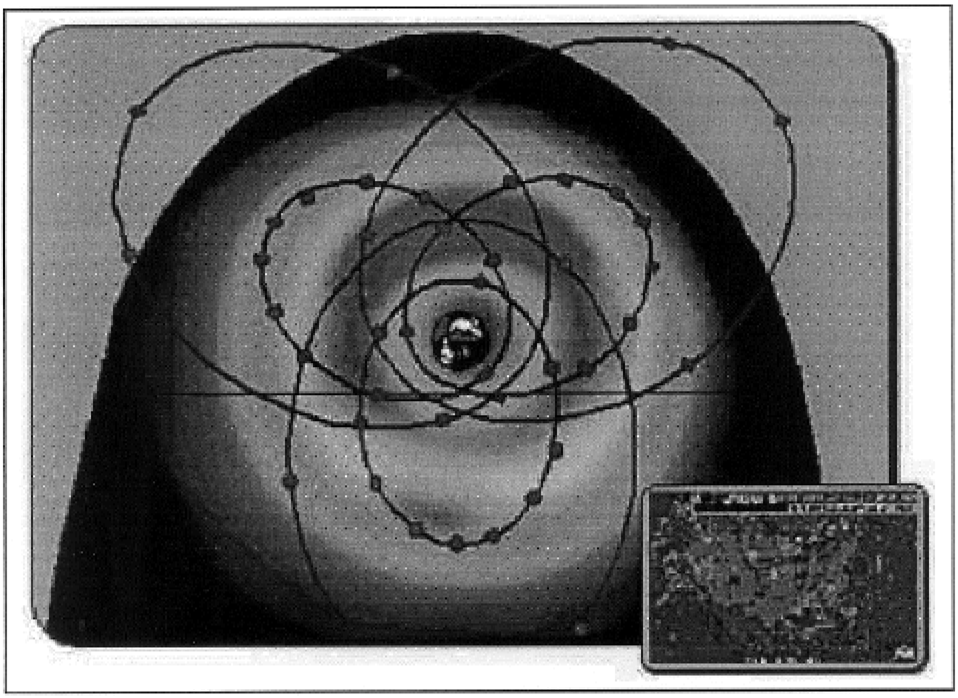

IMS

A constellation of spacecraft situated in six different low-inclination orbits can map the build-up and decay of trapped particles while monitoring the more distant source regions in much the same way as weather stations track storm systems across the Earth's surface.

Technical Requirements:

Microsat technology
Miniaturized instrumentation

LIVING WITH A STAR

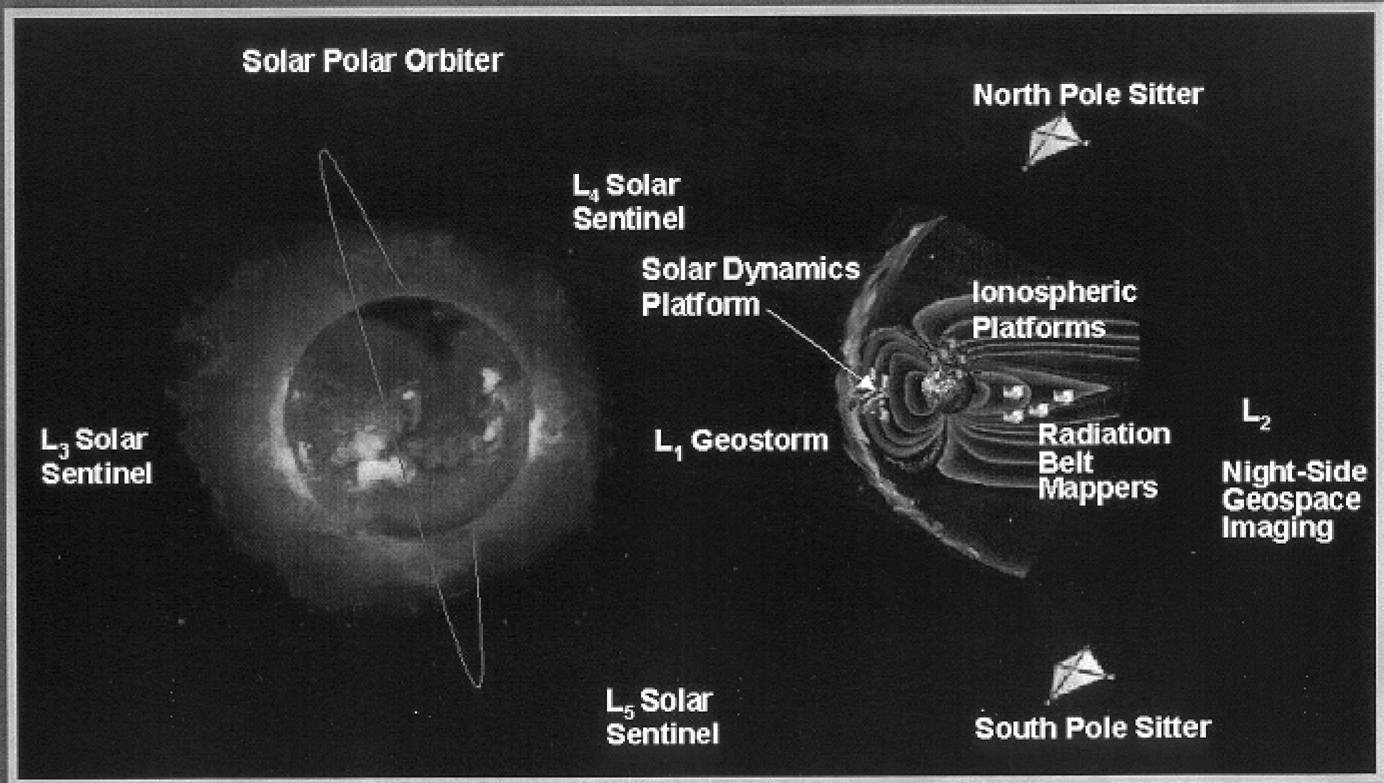

A distributed network of spacecraft will provide continuous observations of Sun-Earth system.